This article was downloaded by:
On: *14 January 2011*
Access details: *Access Details: Free Access*
Publisher *Taylor & Francis*
Informa Ltd Registered in England and Wales Registered Number: 1072954 Registered office: Mortimer House, 37-41 Mortimer Street, London W1T 3JH, UK

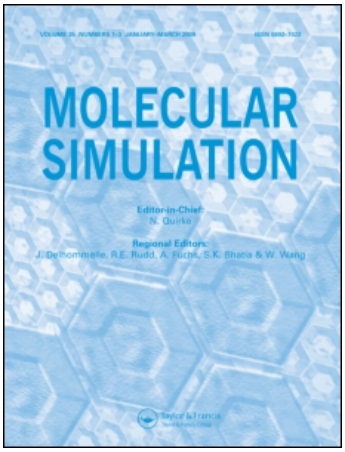

Molecular Simulation
Publication details, including instructions for authors and subscription information:
http://www.informaworld.com/smpp/title~content=t713644482

Molecular Modelling of The Mechanism of Action of Organic Clay-Swelling Inhibitors

A. S. Bains[a]; E. S. Boek[a]; P. V. Coveney[b]; S. J. Williams[a]; M. V. Akbar[a]
[a] Schlumberger Cambridge Research, Cambridge, United Kingdom [b] Centre for Computational Science, Department of Chemistry, Queen Mary and Westfield College, University of London, London, United Kingdom

To cite this Article Bains, A. S. , Boek, E. S. , Coveney, P. V. , Williams, S. J. and Akbar, M. V.(2001) 'Molecular Modelling of The Mechanism of Action of Organic Clay-Swelling Inhibitors', Molecular Simulation, 26: 2, 101 — 145
To link to this Article: DOI: 10.1080/08927020108023012
URL: http://dx.doi.org/10.1080/08927020108023012

PLEASE SCROLL DOWN FOR ARTICLE

Full terms and conditions of use: http://www.informaworld.com/terms-and-conditions-of-access.pdf

This article may be used for research, teaching and private study purposes. Any substantial or systematic reproduction, re-distribution, re-selling, loan or sub-licensing, systematic supply or distribution in any form to anyone is expressly forbidden.

The publisher does not give any warranty express or implied or make any representation that the contents will be complete or accurate or up to date. The accuracy of any instructions, formulae and drug doses should be independently verified with primary sources. The publisher shall not be liable for any loss, actions, claims, proceedings, demand or costs or damages whatsoever or howsoever caused arising directly or indirectly in connection with or arising out of the use of this material.

Molecular Simulation, 2001, Vol. 26, pp. 101–145
Reprints available directly from the publisher
Photocopying permitted by license only

© 2001 OPA (Overseas Publishers Association) N.V.
Published by license under
the Gordon and Breach Science
Publishers imprint.
Printed in Malaysia.

Downloaded At: 18:53 14 January 2011

MOLECULAR MODELLING OF THE MECHANISM OF ACTION OF ORGANIC CLAY-SWELLING INHIBITORS

A. S. BAINS[a], E. S. BOEK[a], P. V. COVENEY[b,*], S. J. WILLIAMS[a] and M. V. AKBAR[a]

[a] *Schlumberger Cambridge Research, High Cross, Madingley Road, Cambridge, CB3 0EL, United Kingdom;* [b] *Centre for Computational Science, Department of Chemistry, Queen Mary and Westfield College, University of London, Mile End Road, London, E1 4NS, United Kingdom*

(Received November 1999; accepted December 1999)

It is well known that the sodium smectite class of clays swells macroscopically in contact with water, whereas under normal conditions the potassium form does not. In recent work using molecular simulation methods, we have provided a quantitative explanation both for the swelling behaviour of sodium smectite clays and the lack of swelling of potassium smectites [1]. In the present paper, we apply similar modelling methods to study the mechanism of inhibition of clay-swelling by a range of organic molecules.

Experimentally, it is known that polyalkylene glycols (polyethers) of intermediate to high relative molecular mass are effective inhibitors of smectite clay swelling. We use a range of atomistic simulation techniques, including Monte Carlo and molecular dynamics, to investigate the interactions between a selection of these compounds, water, and a model smectite clay mineral. These interactions occur by means of organised intercalation of water and organic molecules within the galleries between individual clay layers.

The atomic interaction potentials deployed in this work are not as highly optimised as those used in our clay-cation-water work [1]. Nevertheless, our simulations yield trends and results that are in qualitative and sometimes semi-quantitative agreement with experimental findings on similiar (but not identical) systems. The internal energy of adsorption of simple polyethers per unit mass on the model clay is not significantly different from that for water adsorption; our Monte Carlo studies indicate that entropy is the driving force for the sorption of the simpler organic molecules inside the clay layers: a single long chain polyethylene glycol can displace a large number of water molecules, each of whose translational entropy is greatly enhanced when outside the clay. Hydrophobically modified polyalkylene glycols also enjoy significant van der Waals interactions within the layers which they form within the clay galleries.

*Corresponding author.

In conjunction with experimental studies, our work furnishes valuable insights into the relative effectiveness of the compounds considered and reveals the generic features that high performance clay-swelling inhibitors should possess. For optimal inhibitory activity, these compounds should be reasonably long chain linear organic molecules with localised hydrophobic and hydrophilic regions along the chain. On intercalation of these molecules within the clay layers, the hydrophobic regions provide an effective seal against ingress of water, while the hydrophilic ones enhance the binding of the sodium cations to the clay surface, preventing their hydration and the ensuing clay swelling.

Keywords: Clay minerals; Organic molecules; Clay swelling; Monte Carlo; Molecular dynamics

Downloaded At: 18:53 14 January 2011

1. INTRODUCTION

Swelling clay minerals play an important role in many industrial processes, such as petroleum engineering and catalysis. During oil and gas exploration and production, serious problems are frequently encountered in shale formations, which contain a high fraction of compacted 2 : 1 clay minerals such as smectites. These problems include borehole instability, associated with the uptake of water by smectites from the fluids used during the drilling of wells.

Smectites are comprised of layers of negatively charged mica-like sheets, held together by charge balancing counter-ions such as Na^+ and Ca^{2+}. In the presence of water these cations tend to hydrate, thereby forcing the clay layers apart in a series of discrete steps [3, 4]. A number of studies claim that the sorption of water into the interlayer spacing is mainly determined by the size and charge of the counter-ions [3, 5]; other authors have shown that the net silicate layer charge [6] and charge location [7] play a major role. At increasing relative humidity, smectites adsorb water vapour, and form one-, two- and three-layer hydrates [4, 6, 8]. Cases *et al.*, have found that the swelling process of sodium montmorillonite was isoenthalpic beyond the two-layer hydration state [8]. Zhang and Low on the other hand still observed a decrease of the heat of immersion beyond this state [9, 10]. A number of experiments have yielded insight into the molecular distribution and organisation of interlayer water and cations adsorbed on clay surfaces [11]; these include X-ray [12, 13], infrared [14] and neutron diffraction [15, 16] studies.

Two types of swelling should be distinguished in relation to clay hydration: (i) intracrystalline swelling, involving the adsorption of limited amounts of water in the interlayer spacing, and (ii) osmotic swelling, related to unlimited adsorption of water due to the difference between ion concentrations close to the clay surface and the pore water. The mechanisms of intracrystalline swelling have been described above; osmotic swelling gives rise to macroscopic expansion of the clay. The tendency of

sodium-saturated smectites to swell macroscopically is the principal cause of shale instability in oil well drilling operations and may even lead to collapse of the wellbore. The worldwide cost of wellbore instability problems to the oil industry is estimated to be more than $600 million per year. For this reason, a large research effort has been directed to shale-swelling inhibition. Oil-based drilling fluids do not cause shale swelling, as they exclude additional water from the wellbore. Such fluids however, are usually deemed to be environmentally unacceptable, and are particularly hazardous to marine ecosystems. Therefore current research in this field is focused on improving the properties of water-based drilling muds. One route for the inhibition of shale swelling is the addition of weakly hydrating cations, such as K^+, to the drilling fluid [17]. The potassium ion will replace sodium by cation exchange within the clay, and is found to prevent swelling. Unfortunately, this treatment requires high concentrations of KCl, which is environmentally toxic. Nevertheless, an understanding of the microscopic mechanisms of cation hydration in relation to clay swelling can contribute to the design of new additives for water based muds, which may even be active in the absence of potassium ions. Another attractive route is to develop bio-degradable organic and/or polymer additives for the drilling fluid. The present paper is concerned with this second approach.

Downloaded At: 18:53 14 January 2011

The microscopic structure of water and the distribution of counter-ions near the clay-water interface have long been controversial subjects in colloid science: for example, Sposito and Prost [11] claimed that counter-ion solvation plays a dominant role in the swelling of clays, whereas Low [18] attributed swelling to hydration of the clay surfaces. Accounting for the different properties of sodium and potassium smectites has been one of the most challenging problems in this area. In a recent paper, we have studied the swelling of Li^+, Na^+ and K^+ saturated smectite clays at the molecular level, using Monte Carlo methods and highly optimised force fields which yield quantitative agreement with experimental data on clay swelling [1, 2]. We found that, as the water content is increased, both Li^+ and Na^+ are able to hydrate, thereby becoming detached from the clay surface. In contrast, we found that K^+ ions migrate to the clay surface during these simulations. The natural interpretation of these results is that K^+ ions screen the negatively charged, mutually repelling clay surfaces more effectively than Na^+ and Li^+ ions do. The reluctance of K^+ ions to fully hydrate reduces the tendency of K^+ saturated clays to expand. Our simulations therefore provide a qualitatively satisfying insight into the role of the K^+ ion as a shale swelling inhibitor.

As far as the role of organic clay-swelling inhibitors is concerned, one goal of current research is to achieve oil-based drilling fluid performance

using water-based fluids, that is through the inclusion within a water-based fluid of one or more substances which singly or together inhibit shale swelling to the same degree as an oil-based fluid. At present, the identification of possible additives is normally done by direct testing of a range of commercially available chemical products. As a result of this highly empirical approach, there has been a comparatively poor level of understanding of the mechanisms by means of which many of these additives act. Even the mechanisms of action of existing additives are in large measure unknown.

Low molecular weight polyethylene glycols (PEGs) and more general polyalkylene glycols (PAGs)–also known collectively as polyethers–are increasingly being used as shale-inhibitors in drilling operations, for a variety of reasons. A relatively low concentration of a PEG or PAG is needed in water based fluids, thus making them relatively cheap to use; they do not affect other important fluid properties significantly (such as viscosity, fluid-loss control *etc.*); and they reduce the amount of solids dispersion that can occur. These compounds enhance well-bore stability as they inhibit shale-swelling; their use decreases the rate at which fine shale particulates enter the drilling fluid, although they are not adsorbed in large quantities by clays and so their net consumption rate is low. Moreover, many PEGs also have a low environmental impact.

The purpose of the work described here is to investigate the mechanism of action of PEGs and related compounds on aqueous clay systems using molecular simulation techniques, including in particular energy minimisation, Monte Carlo methods and molecular dynamics. As we shall show, these simulations have enabled us to determine the principal features underpinning this mechanism, and to aid in the rational design of improved clay and shale swelling inhibitors.

Downloaded At: 18:53 14 January 2011

2. CLAY STRUCTURES AND MOLECULES

In the present section, we discuss the basic components which are used in all of our simulations: the structure of the clay mineral, the structures of the molecules used in the initial part of this work, and the model interaction potentials chosen.

2.1. Structural Model of the Clay

In order to examine the kinds of interactions that exist between water, glycols and clays, a representative structure of a clay is required. To the

uninitiated, there is an overwhelming variety of clay minerals [19]. From the point of view of oilfield applications, the smectite group of clays are an obvious choice to study since they are frequently encountered in drilling operations and, as noted above, undergo swelling in contact with water. The smectites consist of 2 tetrahedral silicate layers, sandwiching a single octahedral aluminate layer (hence being referred to as '2:1 clays'). The clay structure we selected for our simulations was based on the commonly studied smectite called montmorillonite. However, one complicating feature of clay chemistry, including montmorillonites, is the variability in chemical composition of notionally identical minerals from one region to another. Compounding this is the fact that montmorillonites are disordered in the planes of the clay layers, and so no structural data is available for montmorillonites in the common international X-ray crystallographic databases. Instead, as a starting point we used the readily available crystallographic data for the mineral potassium muscovite, and manipulated it to generate an approximate representation of montmorillonite. This is a reasonable approximation since the local geometrical features of the muscovite tetrahedral-octahedral-tetrahedral (T-O-T) 2:1 layers are almost identical to those of montmorillonite. However, the metal ion composition within the octahedral layers, where only aluminium ions reside in muscovite, was altered by substitution of some of these Al^{3+} ions with Mg^{2+}, to give the ratio of aluminium:magnesium found in common montmorillonite. The ratio of Al:Mg selected was 3.3:0.7 [19]. Clearly the precise value of this ratio can vary from sample to sample, and this itself may lead to significant effects; we have not, however, considered this issue further here.

To generate an exact replica of the Wyoming-type montmorillonite previously studied [1], it would also have been necessary to replace some Si atoms in the tetrahedral layers by Al, but the required Al:Si ratio is quite low and to implement this in a realistic way would have required a clay structure comprising a rather larger number of atoms than the model we wished to use. As this would have increased the length of what are already very CPU-intensive simulations, we did not include these features in the structure: in the clay terminology, this corresponds more nearly to an 'Otay-type', prototypical montmorillonite (*cf.* also [20]). The periodic clay structure constructed in this way was left with a net negative charge owing to the ion substitutions in the octahedral layers; this was balanced by the insertion of extra interlayer counter-cations, initially potassium (the cation in the original muscovite structure) to maintain overall electroneutrality. The placement of these cations was done in such a way as to preserve symmetry and to mimic the cation positions in muscovite. The unit cell

Downloaded At: 18:53 14 January 2011

formula for the montmorillonite structure we used was therefore:

$$K_{0.69}(Si_{8.00})[Al_{3.31}Mg_{0.69}]O_{20}(OH)_4.$$

The only other counter cation studied in the present work is sodium, which was inserted into identical positions to those occupied by potassium in the anhydrous structure. It is worth emphasising that the exact location and hydration state of these cations in smectite clays are not generally known although our recent modelling work provides answers to such questions [1, 21]. Nevertheless, by starting from the K^+-ion positions in the muscovite crystal structure it is believed that the location of these cations in anhydrous montmorillonite is probably reasonably well represented. Figure 1 is a (001) view of the basic clay structure used in all the simulations reported here. For reference, the colour scheme used in the figures contained in this paper is as follows:

- Grey – Carbon
- Red – Oxygen

Downloaded At: 18:53 14 January 2011

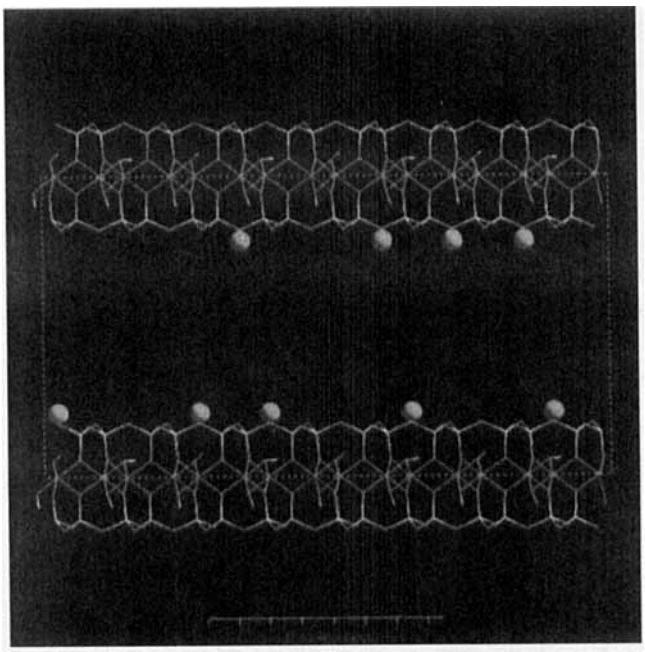

FIGURE 1 The basic three-dimensional montmorillonite clay structure used in our simulations. The dotted blue lines indicate the boundaries of the simulation cell; as described in the text, periodic boundary conditions are applied in all three spatial directions to simulate an effectively infinite solid clay sample. The blue spheres indicate potassium counter-cations. (See Color Plate I).

- Yellow – Silicon
- White – Hydrogen
- Brown – Aluminium
- Green – Magnesium
- Blue – Interlayer potassium counter-cations
- Pink – Interlayer sodium counter-cations

2.2. Molecules Studied Initially

To begin our simulations, we studied the interaction of the clay specified in Section 2.1 with the following three molecules:

- water
- ethylene glycol (EG)
- PEG300 (polyethylene glycol; relative molecular mass 300)

The need for water is self-evident. The two glycol molecules (whose molecular structures are shown in Fig. 2) of widely differing masses were selected principally because of their known and contrasting inhibitive abilities. For example, it is known that EG is a poor clay-swelling inhibitor in low concentrations, although it is more effective at very high concentrations (> 60 wt%), whereas PEG300 is relatively good at preventing shale-swelling at concentrations of approximately 6 wt%. It was hoped that these differences would help us to understand the inhibition process more clearly. In fact, larger molecules such as PEG600 are currently being used in real drilling operations: for reasons of CPU time, we selected a molecule of half this size (PEG300) so that we could perform simulations on an acceptable wall-clock timescale.

Downloaded At: 18:53 14 January 2011

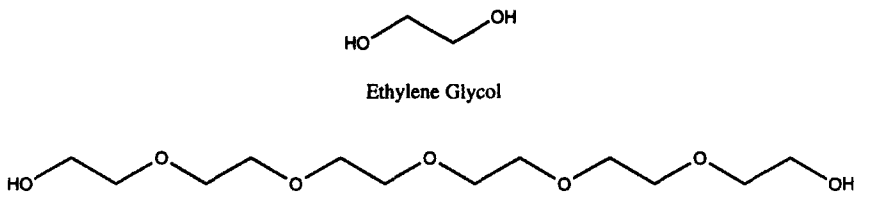

FIGURE 2 The simple glycols used in the initial simulations.

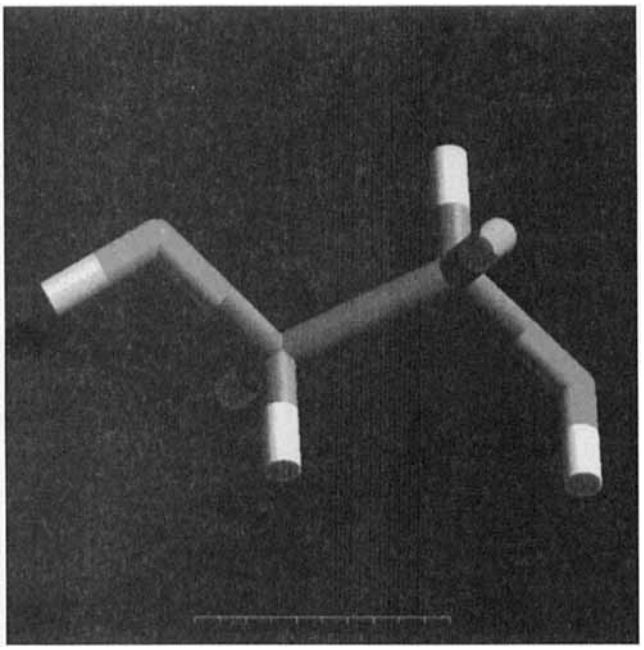

FIGURE 3 An energy-minimised model of ethylene glycol using the MNDO molecular orbital approximation scheme. (See Color Plate II).

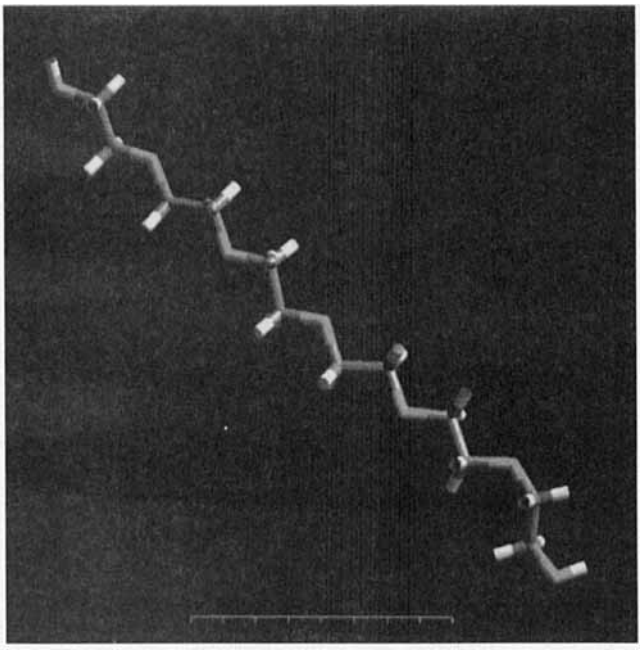

FIGURE 4 An energy-minimised model of PEG300 using the MNDO molecular orbital approximation scheme. (See Color Plate III).

Downloaded At: 18:53 14 January 2011

The ground state energies of all these molecules *in vacuo* were computed using the semi-empirical MNDO molecular orbital approximation scheme [22]; the resultant conformations of EG and PEG300 are shown in Figures 3 and 4. These structures and their associated electronic properties are used in the classical (force field based) calculations which make up our other simulations. (In fact, quite similar molecular properties were obtained when we performed energy minimisation calculations on these same molecules using the Dreiding II force field [23].)

3. SIMULATION METHODS AND POTENTIAL MODELS

In this section, we discuss the potential models and simulation methods used. The simulation techniques used include Monte Carlo and molecular dynamics, described in Sections 3.1 and 3.2. A key element in both of these is the selection of suitable atomistic interaction potentials for the complicated systems currently under investigation; the issues are addressed in Section 3.3.

Downloaded At: 18:53 14 January 2011

3.1. Monte Carlo Simulations

Many of the simulations reported here were performed using a commercially available molecular modelling package [24]. This package contains a grand canonical Monte Carlo code, which uses the Metropolis algorithm [25, 26], and has been designed primarily to simulate molecular gases and vapours (*e.g.*, water and aqueous solutions) interacting with porous inorganic frameworks, such as zeolites. Molecules are treated as rigid bodies, and molecular orientations are stored as quaternions. Our periodic simulation cell consists of two complementary montmorillonite half-layers (Section 2.1) measuring $35.98 \times 20.78\,\text{Å}^2$ (see Fig. 1), with a basal spacing chosen according to the simulations (a typical value being 19 Å). The thickness of one layer is 3.37 Å and periodic boundary conditions are applied in three dimensions. In view of the 3D periodic boundary conditions, the simulations model an infinite stack of clay platelets, which is very similar to those found in real clay minerals. The van der Waals interactions have a cut-off radius of 8.0 Å. Long range electrostatic interactions are calculated by using the Ewald sum method in conjunction with three-dimensional periodic boundary conditions. Previous atomistic clay simulations [20, 1] confirm that the properties of such relatively small simulation cells are still representative of the macroscopic system, and are not influenced by the artificial long-range symmetry of the periodic lattice imposed.

Our simulations were performed in the grand canonical (μVT) ensemble. The volume V and the temperature T of the system are fixed ($T = 300$ K in general, unless otherwise stated) and the simulation reaches equilibrium when the chemical potential μ of the fluid in the external reservoir reaches the same value as that of the molecules sorbed within the clay. We are free to specify the chemical composition of the surrounding vapour; that is, it can be anything from a pure fluid to a mixture of arbitrary chemical composition. This is, in principle, an improvement over our previous simulations [1] although satisfactory equilibration in such a grand ensemble simulation is computationally difficult to achieve, particularly for liquid water, and can need a very large number of MC moves, making it a computationally expensive technique [27]. In fact, this is less of a problem for simulations of systems dominated by short-range interactions, and a large number of ours involving organics fall into just this category; later on, we shall also show that this approach has proved quite successful even in the case of water. Karaborni *et al.*, have also performed (μVT) simulations of water adsorption in a smectite clay [28]. However, these authors failed to find a stable clay bilayer hydrate, which is a common experimental observation. The reason for this is probably an inappropriate choice of the interaction potential for water, in combination with the grand-canonical algorithm.

A Monte Carlo move involves a change in the centre of mass coordinates and the orientation of a randomly selected molecule. In canonical ensemble MC, the general probability of acceptance of a move is:

$$P = \min\{1, \exp(-\Delta U/kT)\} \tag{1}$$

where

$$\Delta U = U_f - U_i. \tag{2}$$

Here ΔU is the internal ('configurational') energy change in moving from initial state i to final state f and k is Boltzmann's constant.

In grand canonical Monte Carlo (GCMC), each molecular component used in a simulation has a specified chemical potential μ. Although in physical terms we envisage the system being simulated as one in contact with an infinite reservoir of a liquid at the appropriate composition, if we make the assumption that the solution (in general a mixture of water and one or more other compounds) behaves ideally, then we can describe the liquid in terms of the behaviour of the composition of the vapour in thermal

Downloaded At: 18:53 14 January 2011

equilibrium with it. In this case,

$$\mu_i(g) = \mu_i^{\ominus}(g) + RT\ln(p/p^{\ominus}), \tag{3}$$

where $\mu_i^{\ominus}(g)$ is the chemical potential of the ith species in its gaseous standard state; p is its vapour pressure; and $p^{\ominus}$ is the vapour pressure of the gas in its standard state (equal to 1 atm). Now, for the ensemble at equilibrium, the chemical potential of the vapour ($\mu_i(g)$) is equal to its chemical potential within the framework ($\mu_i(f)$). Thus

$$\mu_i(f) = \mu_i^{\ominus}(g) + RT\ln p. \tag{4}$$

Put another way, the partial pressure of the vapour i is a measure of its chemical potential,

$$p = [\exp(\{\mu_i(f) - \mu_i^{\ominus}(g)\}/RT)] \tag{5}$$

Initially the clay framework is free of molecules derived from the liquid (or, equivalently, from the vapour); subsequent configurations are produced by one of the following four possible Monte Carlo moves:

(a) *Insertion of a molecule* a molecule is selected at random and randomly inserted into the framework. This new configuration is accepted with a probability given by

$$P = \min[1; \exp(-\Delta U/kT - \ln(kT(1+N_i)/Vp_i))], \tag{6}$$

where N_i is the current number of molecules of component i present in the framework, p_i is the partial pressure of component i in the gas phase, and V is the volume of the cell.

(b) *Destruction of a molecule* a single molecule is randomly removed from the framework and the new configuration is accepted with a probability given by

$$P = \min[1; \exp(-\Delta U/kT + \ln(kTN_i/Vp_i))]. \tag{7}$$

(c) *Translation of a molecule* the centre of mass of a randomly selected molecule in the framework is translated a random distance within a cube of side 2δ (where δ is the maximum step size, see below) and the configuration thus produced is accepted using Eq. (1).

(d) *Rotation of a molecule* a randomly selected molecule in the framework is rotated through a random angle within the range $-\alpha$ to $+\alpha$ (where α is the maximum angular step size). Again the new configuration is accepted using Eq. (1).

Downloaded At: 18:53 14 January 2011

The maximum size of a random translation or rotation of a molecule must be carefully selected: too high a value reduces the probability of a new molecule interacting with the framework and thus slows down the simulation; too low a value also increases the simulation time as it will take longer to generate configurations not similar to the initial one. To determine optimal values in practice requires something of a trial and error approach. In our case, this yielded the following maximum step sizes:

- translation: $\delta = 12$ Å
- rotation: $\alpha = 65°$

These values are automatically rescaled during the simulation in order to minimise the equilibration period needed.

At the start of each simulation, the clay interlayer spacing was set to a value close to and above the experimentally known or anticipated distance. This was necessary to ensure a reasonable probability of insertion, particularly for the larger molecules such as PEG300. Equilibration was judged to have taken place when the average potential energy had reached a constant value. This typically took 3 million Monte Carlo moves which required a calculation time of approximately 60 CPU hours on a Silicon Graphics Indigo2 workstation using an R4400 processor and approximately 40 hours on an R8000 processor.

As stated above, all molecules are treated as rigid in these MC codes. In the case of the molecules described in Section 2.2, we worked with the conformers generated by energy minimisation. Of course, it is quite possible that conformations may change on adsorption, and we have investigated this issue both through the use of molecular dynamics, and by creating 'libraries' of possible conformers which can compete with one another for preferential adsorption on the clay surfaces; these matters are discussed in Sections 3.2 and 5 below.

3.2. Molecular Dynamics Simulations

As noted above, our MC simulations are constrained in that they are carried out at fixed volume, so that they do not enable the clay simulation cell size to vary on adsorption of water or other molecules. Accordingly, we have performed molecular dynamics (MD) in an NPT ensemble on the resulting equilibrated states at a fixed hydrostatic pressure $P = 0.1$ MPa, and with the temperature maintained at $T = 300$ K by the Nosé temperature scaling method [29]. Molecular dynamics was generally carried out following an additional energy minimisation step which is required to reduce unfavourable

Downloaded At: 18:53 14 January 2011

non-bonded atom–atom contacts. MD also enables one to probe any effects due to conformational flexibility which may have been omitted from the GCMC simulations.

As in Section 3.1, periodic boundary conditions are applied in three dimensions. Van der Waals interactions are treated with a cut-off radius of 8.5 Å. Electrostatic interactions were calculated using either the Ewald summation method or a simpler spline cut-off technique (coming in at 8.0 Å and vanishing at 8.5 Å); the latter was preferred for most of our work as it is computationally faster and did not lead to significant errors when compared to the former method (see Section 4.2.3). The integration step size was 1 fs, performed using a modified Verlet algorithm [30].

The MD simulations were run until the clay interlayer spacing had reached a stable value; this in general took no more than 25 ps with a required calculation time of approximately 48 CPU hours on a Silicon Graphics R4400 processor, and 30 CPU hours on an R8000.

In these simulations, none of the atoms were clamped but instead were allowed to move according to Newton's equations of motion within the same force field as used in Section 3.1; see Section 3.3. From our present point of view, the most important result that emerges from these MD simulations is an estimate of the clay interlayer spacing, although in principle other information could also have been extracted, including radial distribution functions and diffusion coefficients.

Downloaded At: 18:53 14 January 2011

3.3. Model Interaction Potentials

The quality of MC and MD simulations is clearly dependent on the choice of the interaction potentials [31]; particularly in the case of hydrated smectite clays, the total interaction energy contains many terms, which are in a subtle balance [1]. In the present case, one would obviously prefer to work with a dedicated clay mineral force field which would aim to capture reliably all the atom–atom interaction potentials for the elements involved. Such a force field is not available, however. Previous work [1] on interlayer water within 2:1 clays has drawn on existing water–water, cation–cation and water–cation interaction potentials and was concerned with the construction of water–clay, clay–clay and clay–cation potentials. This is certainly a step in the right direction for our current work, although the clay–water force field does not include organic molecules in which we are centrally interested. In principle, following our previous research [1], we could hope to draw on the work of Jorgensen *et al.* [32] which has been aimed at providing a systematic set of transferrable intermolecular

potentials (TIPs) for general use. While this approach now includes a wide range of organic species [33], together with cations and water, it is still not sufficiently comprehensive to be of direct use to us.

As a result of the lack of the full range of OPLS (optimized potentials for liquid simulations) parameters needed to specify the potentials for the systems we wish to study, we have been obliged to work with Rappé's so-called 'universal force field' (UFF) [34]. This force field is vaunted as providing a parameterisation of all atomic interactions across the entire periodic table. However, precisely in view of its universality, it is unlikely to compete effectively in terms of accuracy in dedicated applications, such as modelling interactions involving water, a feature which we must bear in mind when interpreting our results later on.

In the universal force field approach [34], the full intermolecular potential energy V is written as a sum of independent contributions:

$$V(r) = V_{\text{el}} + V_r + V_\theta + V_\phi + V_{\text{vdW}}, \tag{8}$$

V_{el} denoting the electrostatic contribution, V_r the vibrational energy, V_θ the bending energy, V_ϕ the torsional energy and V_{vdW} the van der Waals interactions. Non-bonded interactions, V_{nb}, are pairwise additive, involving Coulombic and Lennard–Jones 6–12 terms:

$$V_{\text{nb}} := V_{\text{el}} + V_{\text{vdW}} = \sum_{i \neq j} (q_i q_j / r_{ij} - D_{ij}/r_{ij}^6 + E_{ij}/r_{ij}^{12}) \tag{9}$$

where the sum is over all atomic coordinates and $r_{ij} = |\mathbf{r}_i - \mathbf{r}_j|$. However, all parameters in Eq. (8) are assigned to all atoms individually so that pairwise terms like D_{ij} and E_{ij} in Eq. (9) are computed directly [34]; see Tables I and II respectively.

Given the considerable amount of effort expended in previous work on optimising force fields in these clay systems, particularly for water, it is appropriate to address a few words to the question of whether we can hope that the UFF will be capable of delivering adequate results in the present work. One answer to this is to state that the results obtained by using this

TABLE I Electronic charges, as used in the universal force field

Site	*q(e)*	*Site*	*q(e)*
O	2.30	K	1.16
H	0.71	Al	1.79
C	1.91	Mg	1.78
Na	1.08	Si	2.32

Downloaded At: 18:53 14 January 2011

TABLE II Van der Waals parameters, as used in the universal force field

Sites	D $(kcal\mathring{A}^6/mol)$	$E \times 10^{-3}$ $(kcal\mathring{A}^{12}/mol)$
O	220.6	202.8
H	50.9	14.69
C	685.0	1117.1
Na	42.30	14.9
K	214.8	329.5
Al	8375.6	34728.28
Mg	168.8	64.14
Si	5047.0	15841.1

parameterisation fortuitously appear to be quite reasonable, as we shall show in the current paper. However, in previous work, we have made a comparison between the properties of bulk water predicted using the UFF, Dreiding and TIP3P force fields [35]. These results show that the UFF model is incapable of capturing correctly the experimentally observed features of liquid water, such as density and radial distribution functions; the Dreiding force field does a semi-quantitative job and TIP3P yields almost quantitative agreement. Nevertheless, it is a moot point as to whether the water intercalated within clay structures truly behaves as the bulk liquid, or approximates more closely to a dilute, gas-phase state. Indeed, the present work indicates that the universal force field is adequate for describing the behaviour of these clay–water-organic systems, at least qualitatively and even semi-quantitatively, as we shall see.[1]

Downloaded At: 18:53 14 January 2011

4. SIMULATION RESULTS

The general strategy adopted in the current simulation work should be clear from the foregoing sections. Our general procedure has been to perform Monte Carlo simulations followed by molecular dynamics. The grand canonical MC technique provides us with considerable flexibility in setting up both pure component sorption and sorption from mixtures, such as water and a polyether (as might occur in a drilling fluid). In the work described here, only sodium and potassium counter cations are discussed. Our principal interests are to determine estimates of clay interlayer spacings and to investigate any structuring of intercalates within the interlayer. At a more general level, we wish to understand the mechanism of inhibition of clay swelling by appropriate molecules, so we shall be looking for

[1]In subsequent work, we have in fact made use of a more accurate parameterisation based on the Dreiding force field.

any clues in this direction from the results of our simulations. Overall, we are mainly interested in uncovering such trends as may be apparent, and thus the emphasis of this study is more qualitative than quantitative.

4.1. Canonical Ensemble Simulation Results

Before commencing on a description of the main set of simulation results derived from the application of the grand canonical MC procedure, there was one small group of simulations we wished to consider first. These were three *canonical NVT* ensemble MC simulations with the number of sorbates, N, fixed as one. In separate simulations the three molecules: water, ethylene glycol and PEG300 (see Section 2.2) were sorbed on the periodic clay structure of Section 2.1 for which the clay counter ions had been removed (although in this case the clay template was charge-averaged to zero, for otherwise the codes do not work). The purpose of doing this was to investigate the affinity of these molecules for the clay surface itself, as opposed to the counter-cations. The results are summarized in Table III.

As can be seen from Figure 5, there are no substantial interactions between the single glycol molecule and the surface. The lack of affinity of this molecule for the alumino-silicate layer is not itself surprising: talc, for example, is known to be hydrophobic. There is even repulsion between the negatively charge (P)EO oxygens and the clay surface.

The effect of the counter-cations can be gauged by repeating these canonical MC simulations in the case where the negative charge on the clay slab is balanced by alkali metal cations; see Table IV and Figure 6.

In this case, both EG and PEG300 showed considerable affinity for the surface. As stated earlier, these canonical MC simulations employ rigid molecules, as with the grand canonical version used in this work; one might expect the conformational rigidity to have an effect on the MC process. However, in some molecular dynamics simulations which we have performed on PEG300 following single sorbate canonical MC, we did not observe any significant change in the molecule's conformation, suggesting

TABLE III Canonical ensemble MC simulations of water, ethylene glycol and PEG300 interacting with a single alumino-silicate layer devoid of counter cations

Molecule	*Configurational energy change kcal/mol*
Water	−3
PEG300	−15
EG	−14

Downloaded At: 18:53 14 January 2011

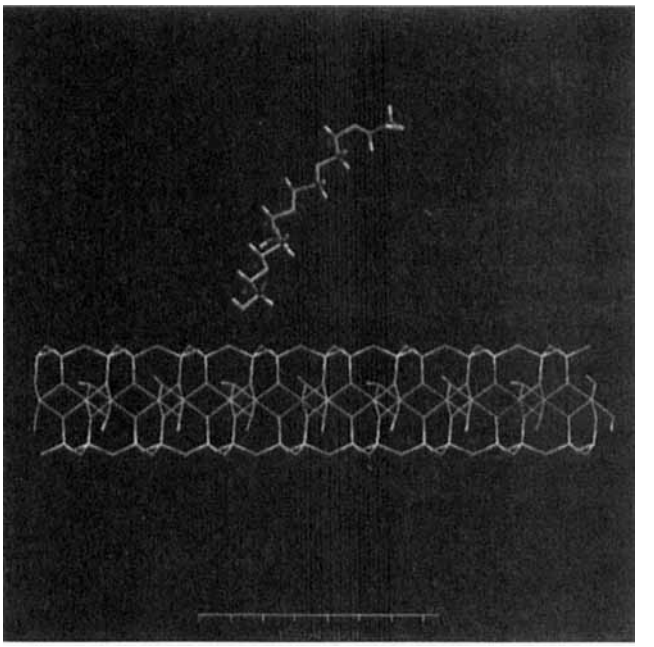

FIGURE 5 Result of a Monte Carlo simulation of one PEG300 molecule interacting with an alumino-silicate layer of montmorillonite in the absence of counter-cations. (See Color Plate IV).

TABLE IV Canonical ensemble MC simulations of water, ethylene glycol and PEG300 interacting with an alumino-silicate clay layer and its accompanying potassium counter cations

Molecule	*Configurational energy change kcal/mol*
PEG300	−68
EG	−28

that the inclusion of internal rotational (and vibrational) degrees of freedom would not significantly affect the conclusions obtained here. This is a conclusion which broadly turns out to hold in all our simulation work. These results suggest that the interaction between the cations and the polar regions of the sorbate molecules is a crucial one in determining the interaction of these hydroxyl-containing compounds with montmorillonite.

Note that, for the case of clay and water shown in Figure 7, we observe the arrangement of the water molecules into two distinct and relatively well ordered layers, a familiar phenomenon in clays which can also be observed when 100% EG and 100% PEG300 are adsorbed in sodium montmorillonite

Downloaded At: 18:53 14 January 2011

Downloaded At: 18:53 14 January 2011

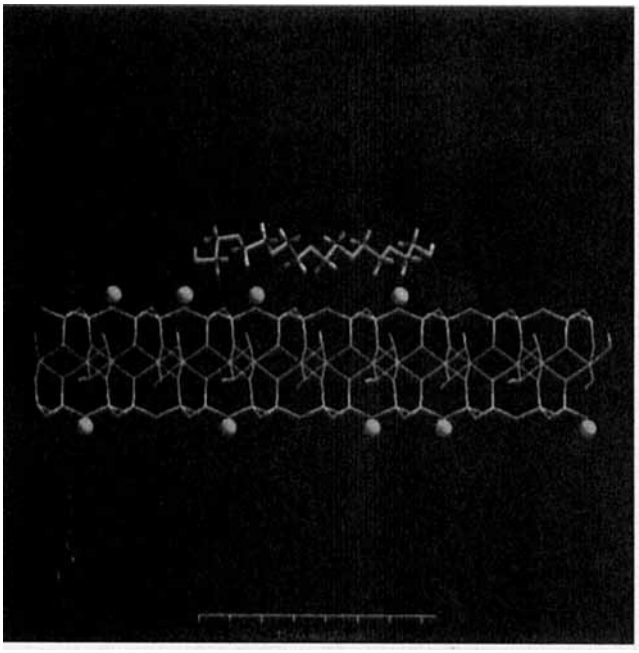

FIGURE 6 Result of a Monte Carlo simulation of one PEG300 molecule interacting with a single alumino-silicate layer of montmorillonite in the presence of potassium counter cations. (See Color Plate V).

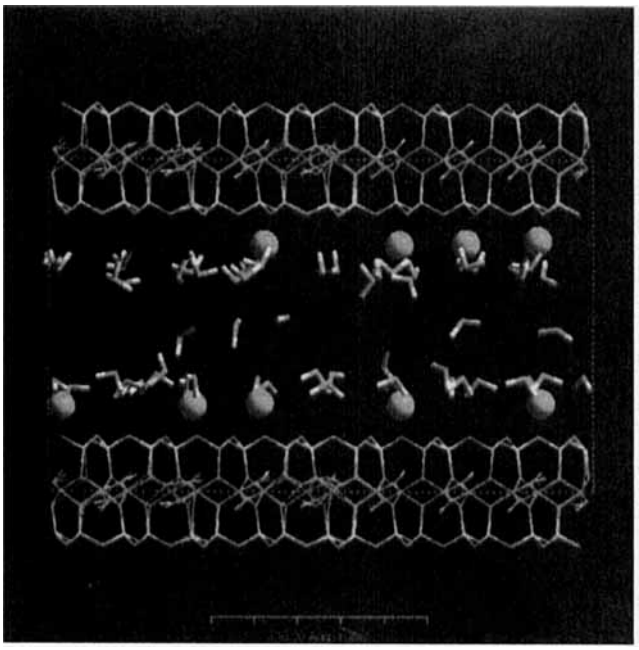

FIGURE 7 Snapshot from an *NPT* molecular dynamics simulation performed on the Monte Carlo equilibrium state of water and potassium montmorillonite. The sodium case is similar. (See Color Plate VI).

TABLE V Data from grand canonical Monte Carlo simulations of glycol-water mixtures adsorbing on potassium montmorillonite

Glycol	*Average loading*		*Internal energy change*
used	*Glycol*	*Water*	*kcal/mol*
H_2O	–	64	−287
PEG300	10	63	−866
EG	42	32	−1141
PEG300	21	–	−957
EG	49	–	−1026

TABLE VI Simulation results for 100% water, EG and PEG300 in sodium and potassium montmorillonites

Sorbate (100%)	*Clay ions*	*Final loading*	*g/100 g of clay*	*Intercalate structure*	*Initial spacing/Å*	*Final spacing/Å*	*Experimental spacing/Å*
Water	K	60	9.1	bilayer	16.0	15.3	15.0
Water	Na	61	9.3	bilayer	19.0	15.3	19.3
EG	K	27	14.3	monolayer	14.0	11.6	17.0
EG	Na	55	29.2	bilayer	19.0	16.5	17.0
PEG300	K	8	19.1	monolayer	14.0	14.0	17.7
PEG300	Na	22	53.1	bilayer	19.0	17.0	17.7

Downloaded At: 18:53 14 January 2011

(Tab. VI). From Table V one sees that the internal energy difference – within the bounds of the many force field approximations involved – between the latter two systems is almost negligible, suggesting that the clay has no enthalpic preference for PEG300. This is, of course, already generally thought to be the case; it confirms that in these cases the inhibition of shale-swelling is almost certainly not an enthalpy-driven process [36, 37].

4.2. Grand Canonical Monte Carlo Simulation Results

In this subsection, we summarise the results obtained from a large number of simulations. We have performed simulations using reservoirs of the pure fluids (water, EG and PEG300) as well as of mixtures (typically ten mole per cent of a polyether in water, a rough approximation to the concentrations used in drilling applications). Molecular dynamics simulations performed after a Monte Carlo run used the NPT ensemble as described in Section 3.2; this maintains the number of particles, pressure and temperature constant throughout the simulation.

4.2.1. Water

Following MC we then ran Nosé NPT canonical dynamics on both systems at 300 K and 1 MPa pressure. On the shortest of timescales (less than a

TABLE VII Simulation results for 10% glycol solutions in potassium montmorillonite

Sorbate (10% *in water*)	*Clay ions*	*Final loading*		*g*/100 *g of clay*		*Intercalate structure*	*Initial spacing*/Å	*Final spacing*/Å	*Experimental spacing*/Å
		Glycol	*Water*	*Glycol*	*Water*				
EG	K	49	10	26.0	1.5	bilayer	18.0	15.3	14.0
PEG300	K	10	48	23.9	7.3	bilayer	19.0	15.3	14.0

picosecond), the most obvious changes are in the dimensions of the unit cell. Over the course of a run, the average shrinkage in the dimensions of the cell (excluding the basal spacing) was 6.1%. The simulations were run until there were no further discernible changes in the periodic cells; this turned out in both cases to be a total time of about 40 picoseconds. The values of the final basal spacings at this time were 15.3 Å for both Na and K respectively (compared with 14.8 Å for sodium–Wyoming montmorillonite, which has tetrahedral substitution [4]); see Figure 7 and Table VII. (It should be noted that the experimental basal spacings listed in Tables VI and VII come from a range of sources, including measurements made in our laboratory on clay minerals whose compositions are similar, but by no means identical with the prototypical Otay clay used in the simulations [38]. For this reason, one should not expect to find quantitative agreement between simulation and experimental results.) Qualitatively speaking we might have anticipated that the sodium basal spacing would be higher than that for potassium. Indeed, inspection of Figure 7 shows that both the Na^+ and K^+ ions have moved away from the clay surfaces, but not by a great deal and indeed by more or less the same amount in both cases.

These data are in reasonable agreement with experimental values (for bilayer adsorption of water); the fact that Na^+ and K^+ behave similarly in this case is probably due to the lack of tetrahedral Al/Mg substitution; our previous work [1] clearly shows that the K^+ ions preferentially remain above such sites on the clay surfaces.

4.2.2. Ethylene Glycol and Polyethylene Glycol

Our GCMC simulations with a reservoir of 100% ethylene glycol produced a bilayer for Na^+ montmorillonite and a monolayer with K^+ montmorillonite. The final loading (number of EG molecules within the simulation cell) with Na^+ was 58; the equivalent system with 100% water rather than ethylene glycol gave a loading of 61. This shows how similiar ethylene glycol is to water so far as the clay is concerned. This same behaviour is also

Downloaded At: 18:53 14 January 2011

evident when a GCMC run is performed with 10% ethylene glycol solution on potassium montmorillonite, when the loadings for ethylene glycol and water are 49 and 10 respectively.

After the GCMC runs using 100% EG, a molecular dynamics simulations using the *NPT* ensemble were carried out on both the bilayer with sodium montmorillonite and the monolayer with potassium montmorillonite. As recorded in Table VI, the EG bilayer contracted from a basal spacing of 19 Å to 16.5 Å and the EG monolayer dropped from 14 Å to 11.6 Å. These results agrees quite closely with the experimental values, also shown in Table VI, although it must be recalled that the experiments were performed on aqueous EG solutions.

The results obtained with reservoirs of 100% PEG300 have relatively well ordered layers and the internal (configurational) energy value shown in Table V, indicating that the clay has no enthalpic preference for PEG300. This is, indeed, already quite widely thought to be the case; it implies that the inhibition of shale-swelling by PEG300 is probably not an enthalpy-driven process [36, 37]. Again, as listed in Table VI, the final spacings after MD are in reasonable agreement with experimental measurements.

Downloaded At: 18:53 14 January 2011

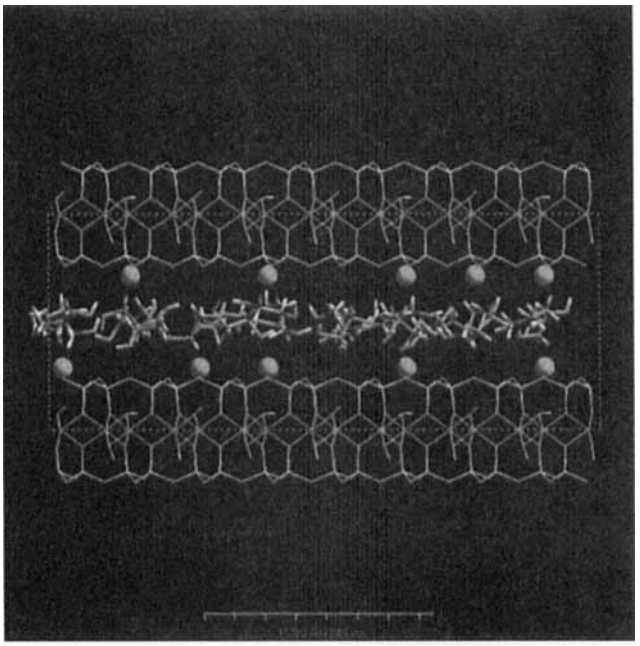

FIGURE 8 Interaction of 100% ethylene glycol and potassium montmorillonite. (See Color Plate VII).

At first sight, after observing the configurational energies and intercalate loadings obtained from the GCMC simulations in Table V for 10% aqueous solutions of ethylene glycol and PEG300 (see also Figs. 9 and 11 respectively), it might be thought that ethylene glycol should be a better shale-swelling inhibitor than PEG300, because more EG molecules insert inside the clay than do PEG. Such a conclusion is, however, clearly at odds with the known experimental properties. Moreover, our PEG300 molecule has six EG residues within it, so a more reasonable comparison requires multiplying the number of PEG300 molecules by six. Then one observes that significantly more EG units are adsorbed within the PEG simulation than for EG sorbing alone. Indeed, in the light of the experimentally observed behaviour, an alternative argument can be propounded based on more general thermodynamic considerations.

If we consider the other important component of the free energy, that is the entropy, we see that its behaviour is likely to be affected to some extent by a process which is implicit in these simulations. One can argue that, since ethylene glycol is very similiar in size and physical properties to water,

Downloaded At: 18:53 14 January 2011

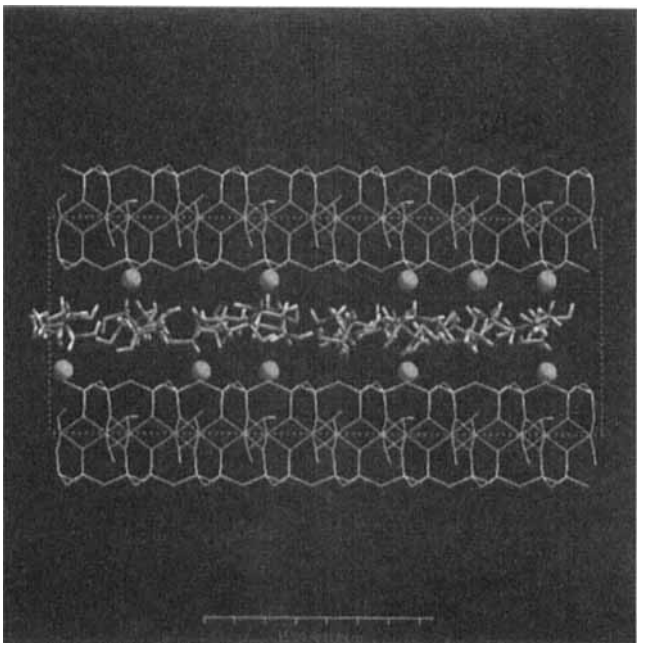

FIGURE 9 Interaction of 10% ethylene glycol solution and sodium montmorillonite. (See Color Plate VIII).

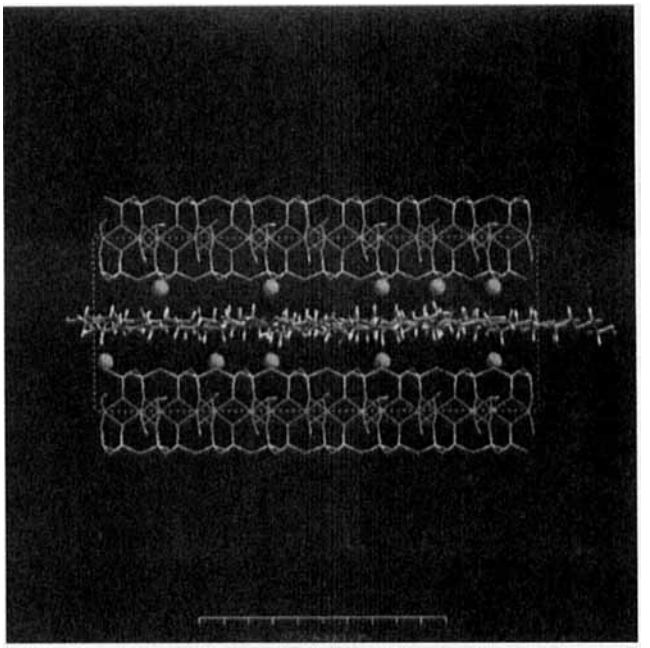

FIGURE 10 Interaction of 10% PEG300 and potassium montmorillonite. (See Color Plate IX).

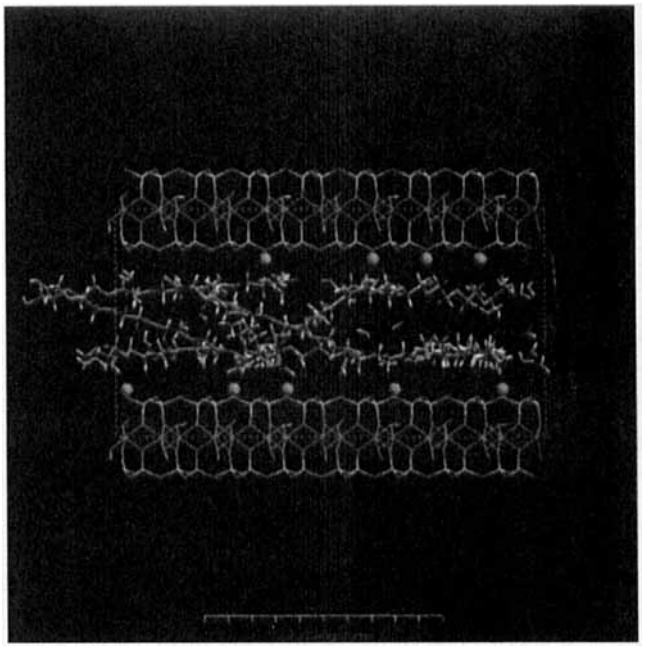

FIGURE 11 Interaction of 10% PEG300 solution and sodium montmorillonite. (See Color Plate X).

Downloaded At: 18:53 14 January 2011

ethylene glycol molecules simply replaces water molecules in the interlayer galleries and thus do not greatly affect the total entropy of the system. However, a single molecule of a long chain glycol such as PEG300 can displace *many* water molecules. Not only are the water molecules that remain within the interlayer spacing more disordered, those that are ejected stand to benefit from a significant gain in entropy. In the interlayer region, the translational degrees of freedom of each molecule are essentially two in number. Outside the lattice, the entropy gain arising from the acquisition of a third translational degree of freedom by the water molecules may well be substantial. On the other hand, so far as the polyethers are concerned, there is some structuring inside the clay, reducing these molecules' entropy, and they must also lose some translational entropy, though this should not be great for large molecules, compared to water. Moreover, a relatively high density of PEG300 molecules occurs within the interlayer galleries because of favourable intermolecular (mainly van der Waals) interactions, leading to increased desorption of water and hence a reduced tendency for the clay to swell. The presence of strong intermolecular forces has already been inferred from infrared spectroscopic measurements [39].

Downloaded At: 18:53 14 January 2011

4.2.3. Neglect of Coulomb Interactions

Previous simulations of certain templating cations which control the topological structures of zeolites have shown that the results obtained are not seriously affected by whether the Coulombic terms are included or excluded [40]. Indeed, if Coulomb interactions can be safely neglected, significant computational savings can be achieved – an important consideration for computations of the size and number reported here. Although at first sight such an approximation seems generally untenable, it leads to important conclusions when successful: in particular, it implies that short-range (van der Waals) interactions furnish the dominant factors governing the processes in question, and may even suggest that a system's behaviour is mainly controlled by geometrical features.

As a check on the relative importance of the Coulomb interactions in our clay systems, we performed two sets of simulations for comparison; in the 'standard' set which was always computed (as described in Section 3.3), all the terms displayed on the right hand side of Eq. (8) were included, whereas in the second smaller number of simulations, the Coulomb interactions V_{el} were omitted. We found that the results obtained were similar for both cases: for Monte Carlo simulations, comparable results from each set

showed the same loadings (numbers of sorbed intercalates); when *NPT*-ensemble molecular dynamics was performed, the resulting simulation cell parameters and in particular the basal or d spacings were again similar (albeit not in precise quantitative agreement). Thus we conclude that intercalate sorption within these clays is controlled by non-Coulombic interactions. Since it is the non-bonded interactions that contribute to the clay-intercalate interaction energy (see Eq. (9)), it follows that the dominant clay-intercalate interactions are the van der Waals forces V_{vdW}. Our interpretation is that the Coulomb interactions are more or less screened away within the interlayer galleries because the counter cations shield the sites of negative charge density within the clay framework itself. This behaviour is in contradistinction with that found in the case of layered double hydroxides, where no such screening mechanism exists and one needs to handle the Coulomb interactions with great care [41].

4.2.4. The Role of Helical PEG Conformers in Sorption

Some authors have proposed that the conformation of oligomeric polyethers (such as PEG300) is helical when they are sorbed into clays [42, 43]. One reason for this suggestion comes from the observation that the solid-state conductivity of such clay-intercalates is anomalously high, thus indicating that there are energetically favourable ion channels within the galleries. These authors inferred that the ion channels are located within the helices of the polyether intercalates. We have investigated this proposal computationally by setting up the sodium montmorillonite model (Fig. 1) in such a way that the Na^+ ions were initially in collinear arrangements located equidistant from the two well-separated clay layers inside the simulation cell, so arranged to maximally encourage the sorbing linear helical conformers to wrap around these cations. When grand canonical Monte Carlo simulations were performed upon this clay using PEG300 as the sorbate in a rigid helical conformation of diameter wide enough for Na^+ to insert comfortably, the PEG300 showed no affinity for the Na ions and a strong reluctance to insert at all. When competitive GCMC runs were performed involving both linear and helical conformers, only the linear ones inserted. According to the picture that emerges from our work, the highly conducting ion channels are more likely to be ones arising from the spacing between the clay surfaces and the intercalate sheets, where the counter cations are most likely to reside. The environment experienced by these mobile cations, sandwiched between clay and polyether, is very similar to that which would be found inside a polyether helix.

Downloaded At: 18:53 14 January 2011

5. SOME NOVEL CLAY SWELLING INHIBITORS

In this section we shall outline the features of several structurally more complicated compounds that show clay and shale swelling inhibition properties. We have divided these into two classes – polyethers and polyhydroxyethers (polyethers with attached hydroxyl groups). It should be noted that we use the term "polymer" in a loose sense, as our molecules have relatively short chains and could more properly be described as oligomers. The use of relatively small polymers was necessary in order to avoid impractically long computation times, and in some cases models of cut-down versions of commercial products have been used (as for example in the case of DCP101, Section 5.1.1). For convenience, we gather here a list of the abbreviations we shall use for describing these molecules in the remainder of this paper:

Alkylene groups

- EO – Ethylene Oxide
- PO – iso-Propylene Oxide
- BO – iso-Butylene Oxide

Polyethers

- DCP101 – A polyalkylene glycol copolymer made up of EO and PO units
- EO/BO – A polyalkylene glycol copolymer made up of EO and BO units
- Pluronic – Although this is a term used to describe a wide class of polymers, we use it here to refer to the polyalkylene glycol block copolymer version of EO/BO

Polyhydroxyethers

- GlycerolEO – A glycerol-based polymer with terminal EO chains
- SorbitolPO – A sorbitol-based polymer with terminal PO chains
- SorbitolBO – A sorbitol-based polymer with terminal BO chains
- Lotibros – An adaptation of SorbitolPO, in which the positioning of the groups is reversed, that is the hydroxyl groups are on the exterior and the PO groups on the interior of the molecule
- Biglotibros – A longer version of Lotibros with more exterior (terminal) hydroxyl groups

The results of the simulations involving these molecules are summarised within this section at various points in Tables VIII – X, as well as the graphs in Figures 22 – 24.

Downloaded At: 18:53 14 January 2011

TABLE VIII Simulation results for 100% glycol in sodium and potassium montmorillonites

Sorbate (100%)	*Clay ions*	*Final loading*	*g/100 g of clay*	*Intercalate structure*	*Initial spacing/Å*	*Final spacing/Å*	*Experimental spacing/Å*
DCP101	K	7	19.2	monolayer	14.0	12.4	17.7
DCP101	Na	18	49.9	bilayer	19.0	17.0	17.7
EO/BO	Na	16	50.1	bilayer	19.0	17.1	17.9
Pluronic	Na	16	53.8	bilayer	19.0	17.4	–
GlycerolEO	Na	21	69.1	bilayer	19.0	19.2	–
SorbitolPO	Na	17	64.3	bilayer	19.0	18.9	17.4
SorbitolBO	Na	15	64.0	bilayer	19.0	19.2	–
Lotibros	Na	18	68.1	bilayer	19.0	19.2	–
Biglotibros	Na	18	82.3	bilayer	19.0	19.4	–

TABLE IX Simulation results for 20% DCP101 solutions at two temperatures in potassium montmorillonite

Temp. /K	*Clay ions*	*Final loading*		*g/100 g of clay*		*Intercalate structure*	*Initial spacing/Å*	*Final spacing/Å*
		Glycol	*Water*	*Glycol*	*Water*			
300	K	10	40	27.7	6.2	bilayer	19.0	16.0
330	K	14	27	38.8	4.2	bilayer	19.0	16.5

TABLE X Simulation data used in graphs. Data apply to sorbates in sodium montmorillonite

Sorbate (100%)	*Mol. wt. g/mol*	*Adsorbed amt. g/100 g clay*	*Density g/cm³*	*Spacing Å*
Water	18	9.3	0.22	15.3
EG	62	29.2	1.42	16.5
PEG300	282	53.1	1.84	17.0
DCP101	324	49.9	1.74	17.0
EO/BO	366	50.1	1.84	17.1
Pluronic	394	53.8	1.72	17.4
GlycerolEO	384	69.1	1.85	19.2
SorbitolPO	443	64.3	1.74	18.9
SorbitolBO	499	64.0	1.74	19.2
Lotibros	443	68.1	1.84	19.2
Biglotibros	535	82.3	2.17	19.4

5.1. Polyethers

Diagrams of these models can be found in Figure 12.

5.1.1. DCP101

Our experimental colleagues have been looking at a number of mixed "EO/PO" glycols – that is, random copolymers comprising ethylene oxide

Downloaded At: 18:53 14 January 2011

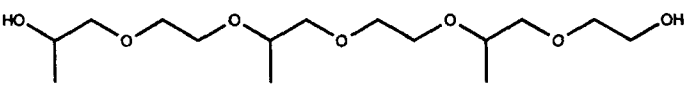

DCP101

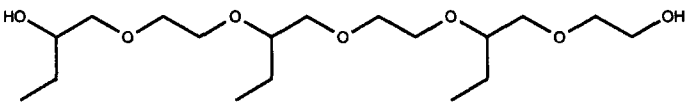

EO/BO

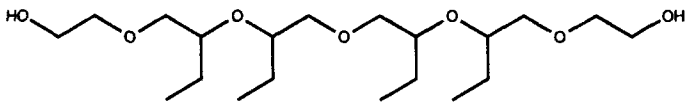

Pluronic

FIGURE 12 Polyethers used in our simulations.

Downloaded At: 18:53 14 January 2011

and iso-propylene oxide sections. One particular example is the commercial product called DCP101, which has a molecular mass of 630 g/mol [44] and exhibits a cloud point at 35°C [48]. In our simulations, we have used a half-sized version of this with regularly alternating EO and PO groups. This differs from PEG300 in having a distribution of hydrophobic methyl groups on every other first carbon in the ethylene oxide linkage.

Our model of DCP101 has a similiar mass to that of PEG300, and the same chain length. As with PEG300, we computed a ground state *in vacuo* conformation for DCP101 using the semi-empirical MNDO molecular orbital approximation scheme [22]. We also employed molecular dynamics using the canonical (NVT) ensemble to generate more conformers at 300 K, and finally we crafted a linear conformer ourselves in which all the methyl groups were in an eclipsed conformation. We then built a 'library' of three conformers of the DCP101 molecule: the artificially constructed linear conformer, an MNDO molecular-orbital-derived conformer and an MD conformer. A competitive grand canonical Monte Carlo simulation was performed using the usual clay structure (see Section 2.1) and these three model DCP101 conformers. (A similar procedure has been advocated by [45, 46] in a different context.) We found that the *linear* conformation of DCP101 inserted in preference to the other conformers, indicating that these molecules show a preference for insertion as rigid rods, although

their energetically preferred conformations externally – *in vacuo* or in solution – are non-linear. The reason for this preference for sorption of the linear conformer appears to be due to optimal packing in this constrained environment and hence optimal van der Waals interactions in this case.

For these reasons, the linear model DCP101 conformer was used as the sorbate for all further DCP101 simulations, and we have also used linear models in the other simulations for the same reasons. We performed grand canonical Monte Carlo on both the sodium and the potassium montmorillonite with 100% DCP101 to produce a bilayer with sodium montmorillonite and a monolayer with potassium montmorillonite. The bilayer result, as shown in Figure 13, is particularly interesting in that the methyl groups point towards each other, creating a hydrophobic barrier which prevents insertion of water. These strong hydrophobic van der Waals interactions are only present in that conformer which has the methyl groups in an eclipsed arrangement, no doubt at least partially accounting for why it enjoys preferential sorption over other possible conformers. The number of model DCP101 molecules in the monolayer and the Na^+-bilayer was 7 and

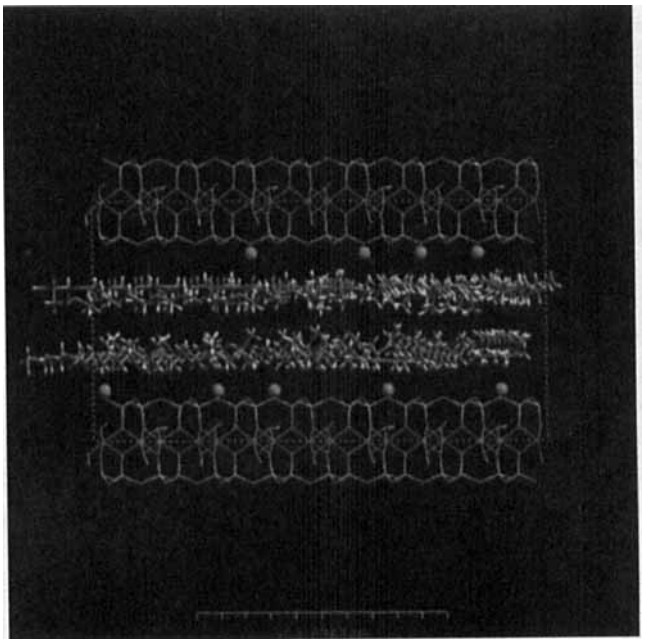

FIGURE 13 Interaction of 100% DCP101 and sodium montmorillonite. (See Color Plate XI).

Downloaded At: 18:53 14 January 2011

17 respectively, similiar to those for PEG300. As normal, we performed molecular dynamics on these models using the *NPT*-ensemble, when the bilayer basal spacing compressed from 19 Å to 17.0 Å, not far from an experimental value of 17.7 Å reported on a related but different clay mineral [38]. The K^+-monolayer contracted from 14 Å to 12.4 Å in MD.

It will be recalled that the presence of a cloud point implies that the aqueous DCP101 system has a *lower* critical consolute temperature (35°C). Thus, at temperatures below this value, the system behaves as a single, homogeneous, phase while above this value there is phase separation into immiscible water-rich and DCP101-rich phases. Two simulations were carried out to observe any features that might be reminiscent of the cloud point behaviour in DCP101: one simulation was performed at 300 K and another at 330 K. (However, it must be remembered that our half-sized version of DCP101 obviously would *not* have the same physical properties, and in particular the same cloud point temperature, if it has one at all, as does true DCP101.) Both fluid reservoirs were made up of 20% DCP101 solution and a grand canoncial Monte Carlo run was executed. The simulation at 300 K produced a water : DCP101 loading ratio inside the clay layers of 34 : 9 while the simulation performed at 330 K gave a ratio of 22 : 11. This represents a modest increase in the proportion of DCP101 inserting at the higher temperature, but cannot be described as in any way dramatic. One can conjecture that at 330 K the lower number of intercalated water molecules compared to that at 300 K is due to the increased self-clustering of the DCP101 at 330 K. One proposed explanation for this phenomenon is that the hydrophobic interactions between DCP101 molecules become relatively stronger as the temperature is increased, while the long-range order in the structure of liquid water is correspondingly reduced. However, it is more likely that the proportion of non-polar conformers increases with increasing temperature, making DCP101 less soluble then [47]. Experimentally, however, no significant change in the efficiency of DCP101 as an inhibitor could be detected above the cloud point [48] and this seems to be broadly consistent with our simulation results.

It should be noted that certain oil companies have advocated the notion of "thermally-activated mud emulsions", based on the premise that the drilling fluid additives should have dramatically enhanced inhibitory properties above their cloud points. Neither the experimental nor the simulation results offer much credance for this idea. This gives additional credibility to our opinion that the mechanism of action of these inhibitors is through intercalation in the galleries, rather than on the scale of complete clay tactoids, which are of a length scale comparable with the DCP101 clusters.

Downloaded At: 18:53 14 January 2011

5.1.2. EO/BO and Pluronic

Colleagues at Schlumberger Cambridge Research have also been studying "EO/BO" glycols, which consist of a mixture of ethylene oxide and isobutylene oxide linkages. We have constructed two molecules of this general form; one is a copolymer with alternating EO and BO groups and the other is a block copolymer which contains a central section of BO groups with EO groups at both ends (which we shall refer to as a Pluronic); see Figure 12. Both of these have been designed with a similar chain length to the half-sized version of DCP101 we employed above. Inspection of the structures in Figure 12 shows that the EO/BO molecule is identical to the DCP101 molecule, except that the methyl side groups of DCP101 have been replaced by ethyl groups.

We carried out grand canonical Monte Carlo simulations using our Otay sodium montmorillonite as the clay template. The loading of the EO/BO intercalate was 16, producing a bilayer, and after molecular dynamics under NPT the basal spacing equilibrated at 17.1 Å. The Pluronic gave the same loading, and 17.4 Å for the spacing after MD. These results are obviously very similar, but certain trends can be discerned – as with all our simulations – which will be discussed in more detail in Section 5.3. At the most basic level, the results we have obtained here show a similar mechanism of action to that observed with the previous oligomers such as PEG300 and DCP101, and help to explain the effectiveness of these EO/BO molecules as clay swelling inhibitors. The EO/BO compound had improved properties compared with DCP101 in experimental tests [48]; this is entirely expected since it has enhanced hydrophobicity.

Downloaded At: 18:53 14 January 2011

5.2. Polyhydroxyethers

In this subsection, we consider a broader range of potential inhibitors, derived from the previous series of molecules but with the added ingredient of one or more hydroxyl groups within the chain. Some of these new compounds have been studied at Schlumberger Cambridge Research. The complete set of molecules we have studied using molecular modelling methods, which is wider in terms of structures probed than the experimental materials, is shown in Figure 14. In all of the simulation reported in this section, we have only performed sorption studies using sodium montmorillonite.

5.2.1. GlycerolEO

The first of the hydroxypolyethers we considered was based on a glycerol residue in the centre of polyether chain which gave the molecule a single

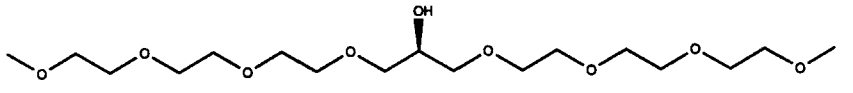

GlycerolEO

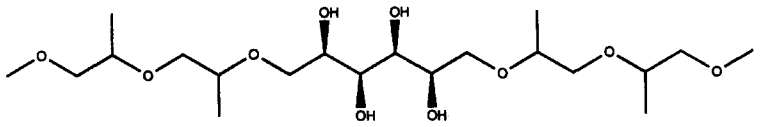

SorbitolPO

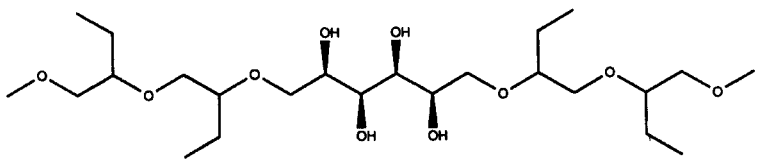

SorbitolBO

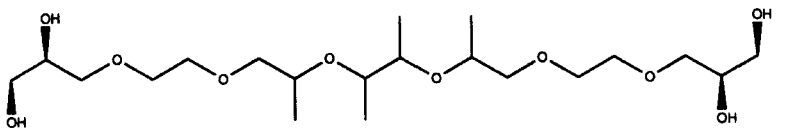

Lotibros

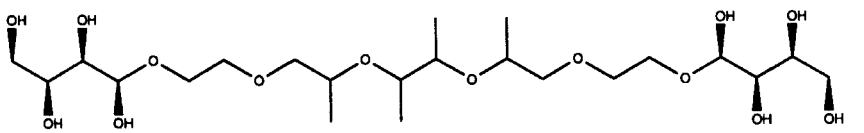

Biglotibros

FIGURE 14 Polyhydroxyethers used in our simulations.

hydroxyl group. We might expect that, as a result of the presence of this hydroxyl group, which may show a relatively greater attraction to the sodium ions than the ether oxygen atoms of the polyethers (PEGs and PAGs), the molecule would adsorb more strongly than previous polymers. As the chain does not have any additional side groups, we would expect that relatively close packing of intercalate molecules would be possible (*cf.* PEG300).

Downloaded At: 18:53 14 January 2011

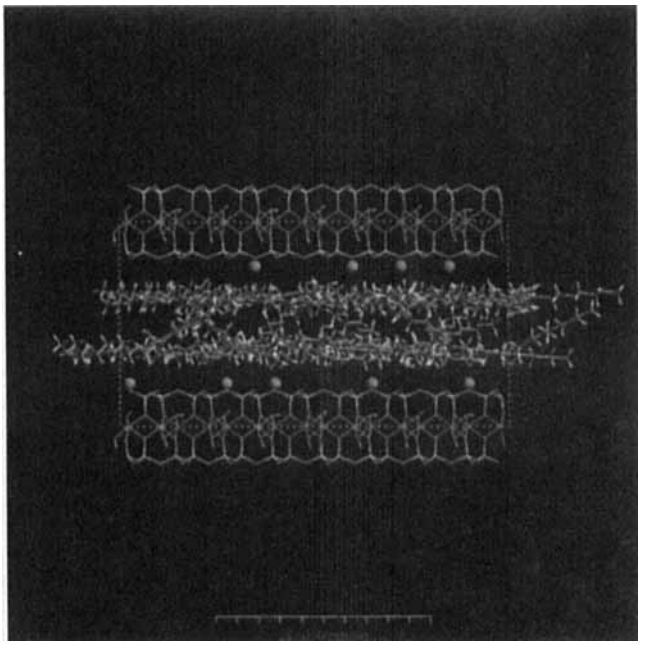

FIGURE 15 Snapshot from an equilibrated GCMC simulation of 100% GlycerolEO and sodium montmorillonite. (See Color Plate XII).

Downloaded At: 18:53 14 January 2011

Grand canonical Monte Carlo followed by *NPT* molecular dynamics simulations were performed using a reservoir comprising a 100% pure linear conformer as before, giving a loading of 21 and a basal spacing of 19.2 Å after MD equilibration. It can be seen from Table VII that the loading (and mass per gram of clay) of GlycerolEO adsorbed are significantly higher than for any of the previous molecules studied. This is an indication that the GlycerolEO molecule does indeed adsorb relatively strongly and packs effectively within the clay galleries. This comparatively dense packing is probably the reason why the layer spacing does not decrease as in the previously reported MD simulations. (Although significant $Na^+ - OH^-$ interactions are not evident in Figure 15, this is probably due to inadequacies in the UFF parameterisation (see Section 3.3), which models these interactions rather poorly.)

5.2.2. SorbitolPO

The second molecule we considered was a sorbitol derivative, as close in structure to what is known of the Terralox 3700 derivative (actually a 70%

Terralox 3700, 30% water mixture) used in some oilfield drilling fluids. Our model has the sorbitol unit at the centre with two PO chains attached to its two terminal OH groups, leaving the four remaining hydroxyl groups of the sorbitol fragment orientated on the opposite side of the molecule to the methyl groups of the PO residues. This has the effect of making one side of the molecule relatively more hydrophilic and the other side relatively more hydrophobic. Figure 16 shows these details of the conformation.

The simulations gave 17 for the final sorbate loading after GCMC, and 18.9 Å for the equilibrated layer spacing after MD. These data are comparable to the results for GlycerolEO (Section 5.2.1) but, more importantly, it can be seen from Figure 17 that the majority of hydroxyl groups are orientated towards the cations, while the methyl groups point away from the clay surface into the interlayer region, creating a predominantly hydrophobic region (similar to DCP101 – see Section 5.1.1). As discussed with DCP101, this region can then act as a barrier to ingress of any water molecules. This effect is most evident in Figure 18 which shows a Monte Carlo simulation that was halted after two molecules had adsorbed into the most preferred positions.

Downloaded At: 18:53 14 January 2011

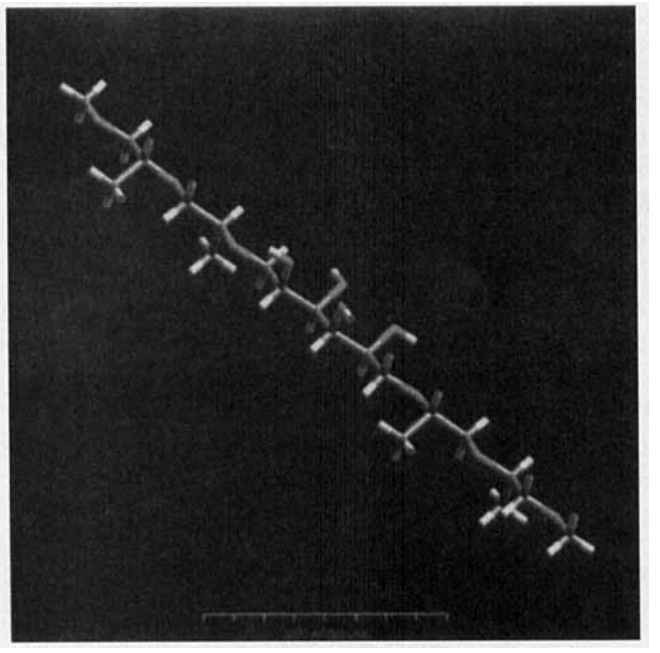

FIGURE 16 The linear conformation of the SorbitolPO oligomer employed in our grand canonical Monte Carlo simulations. (See Color Plate XIII).

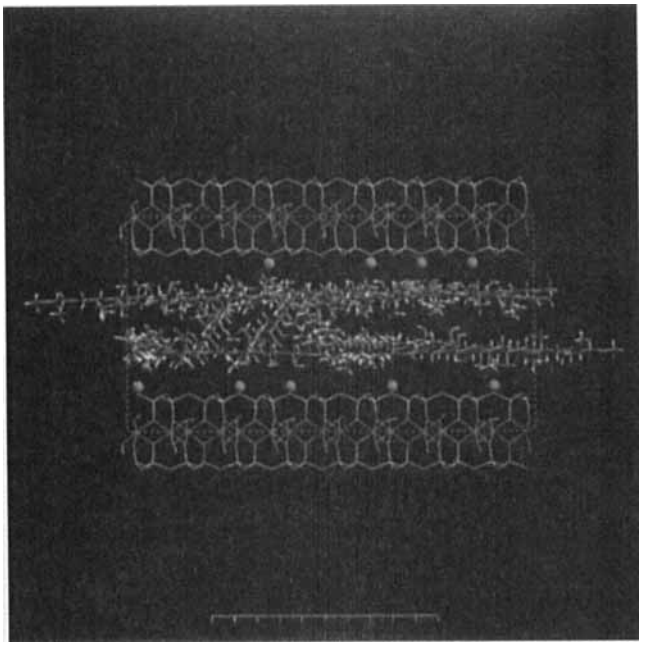

FIGURE 17 Snapshot from an equilibrated grand canonical MC simulation of 100% SorbitolEO and sodium montmorillonite. (See Color Plate XIV).

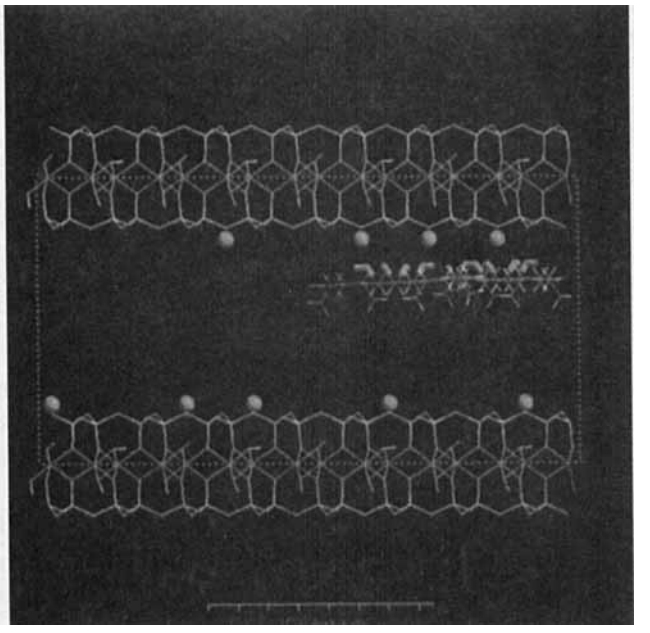

FIGURE 18 Two molecules of SorbitolPO adsorbed on sodium montmorillonite, after a few moves in a grand canonical Monte Carlo simulation. The sorbitol hydroxyl groups have been enhanced for improved visibility. (See Color Plate XV).

Downloaded At: 18:53 14 January 2011

We believe that the stability of the smectite clays in the presence of these particular molecules is due to the fact that they bind the Na^+ ions tightly onto the clay surface from above, making them behave more like K^+ ions [1]; note that these additives achieve good inhibitory performance *without* the need for KCl solution.

5.2.3. SorbitolBO

We then made modifications to the model of SorbitolPO to create a molecule which we call SorbitolBO. This now has butylene oxide residues instead of propylene oxide ones, so the methyl groups of SorbitolPO are replaced by ethyl groups in SorbitolBO. These changes are analogous to those carried out in making EO/BO from DCP101 (see Section 5.1.2).

After we performed GCMC and molecular dynamics simulations on this molecule with sodium montmorillonite, we obtained values of 15 for the intercalate loading and 19.2 Å for the layer spacing. These are similar to those for SorbitolPO; the hydroxyl groups line up as before and the ethyl groups protrude into the interlayer region. Again, this has the desired effect of producing a more hydrophobic interlayer region, and hence an improved barrier to water compared with PEG300. In agreement with expectations, experiments showed that SorbitolBO indeed performs better than SorbitolPO [48].

5.2.4. Lotibros

We have already seen that the two sorbitol-based derivatives adsorb strongly and produce orientations within the clay interlayer which are favourable for their known inhibitory properties. To explore these structure-activity relationships further, we made more extensive modifications to these models for further study. Both the GlycerolEO and the sorbitol-based molecules have a central section of hydrophilic hydroxyl groups and hydrophobic groups (PO or BO residues) towards the two ends of the molecule. We constructed two molecules where this arrangement was reversed, so that the hydrophilic groups were at both ends of the molecule and the hydrophobic groups in the centre. The first of these is what we call "Lotibros".

Lotibros was made by taking SorbitolPO, cutting it in half, and reconnecting the two halves at the opposite ends. This gave a molecule with two hydroxy groups at each end, and four methyl groups in the centre. We then performed GCMC followed by molecular dynamics simulations. The final loading was 18, and the equilibrium basal spacing was found to be

Downloaded At: 18:53 14 January 2011

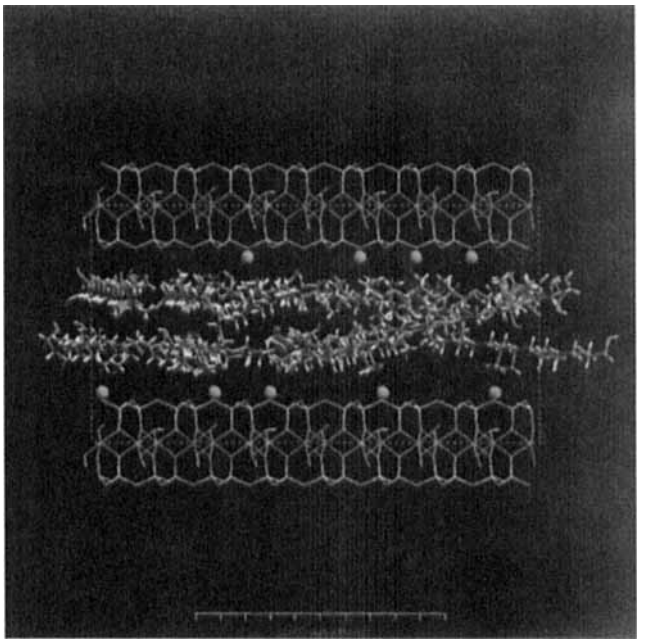

FIGURE 19 Snapshot from an equilibrated grand canonical MC simulation of 100% Lotibros and sodium montmorillonite. (See Color Plate XVI).

Downloaded At: 18:53 14 January 2011

19.2 Å. The loading for Lotibros is very similar to that of SorbitolPO, but the layer spacing is a little higher. It can be seen in Figure 19 that the intercalated Lotibros molecules do not form such a distinct bilayer as did the SorbitolPO: there are now more molecules "crossing-linking" between the clay layers. This is not unexpected because we have already seen in the case of SorbitolPO that the hydrophilic (OH-rich) portions of these molecules are strongly attracted to the sodium counter cations. As these hydroxyl moieties are now grouped in pairs, at both ends of one and the same extended molecule, it is clearly possible for them to be attracted to the counter cations residing in different layers, and hence form a bridge between two adjacent layers. The location of the various functional groups along the backbone is therefore an important structural feature of shale swelling inhibitors (*cf.* Section 5.2.5).

5.2.5. Biglotibros

A further variant of Lotibros is a molecule in which the half-sorbitol groups on the ends are replaced with full sorbitol groups. This gives a new molecule

with four hydroxyl groups at each end rather than merely two, as well as increasing its overall size, as can be clearly seen in Figure 20. We call this molecule Biglotibros.

The results of GCMC followed by MD show the intercalate loading per simulation cell to be the same as Lotibros at 18, and the final layer spacing a little greater at 19.4 Å. However, it should be noted that although the loading is the same, the mass of Biglotibros is greater than that for Lotibros, so the mass of sorbate in the interlayer is greatly increased. This indicates dense packing of the Biglotibros molecules. Examining Figure 21, it is evident that a rather more well defined bilayer has been formed by Biglotibros than by Lotibros. The orientation of the molecules within the galleries is more favourable too, with most of the hydroxyl groups close to the clay counter cation layers, leaving the methyl groups pointing into the interlayer.

Note that although no experiments have been performed using this molecule (nor with Lotibros discussed in Section 5.2.4 above), which were not commercially available, we expect that the stability of such

Downloaded At: 18:53 14 January 2011

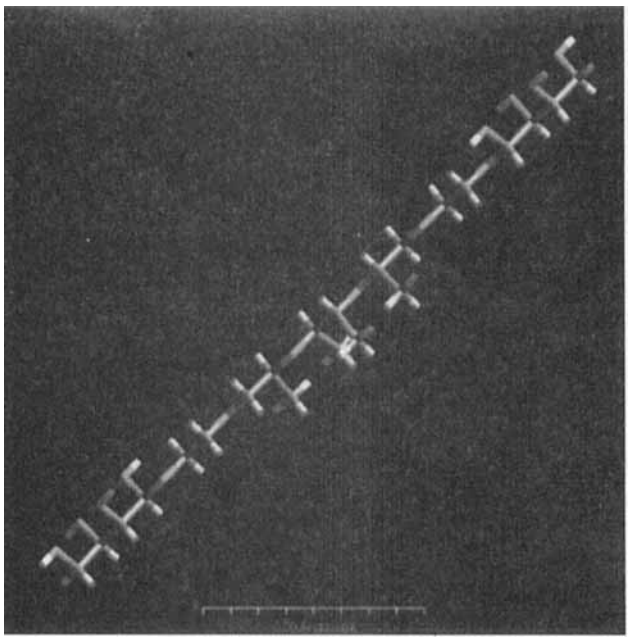

FIGURE 20 The linear conformation of the Biglotibros oligomer employed in our grand canonical Monte Carlo simulations. (See Color Plate XVII).

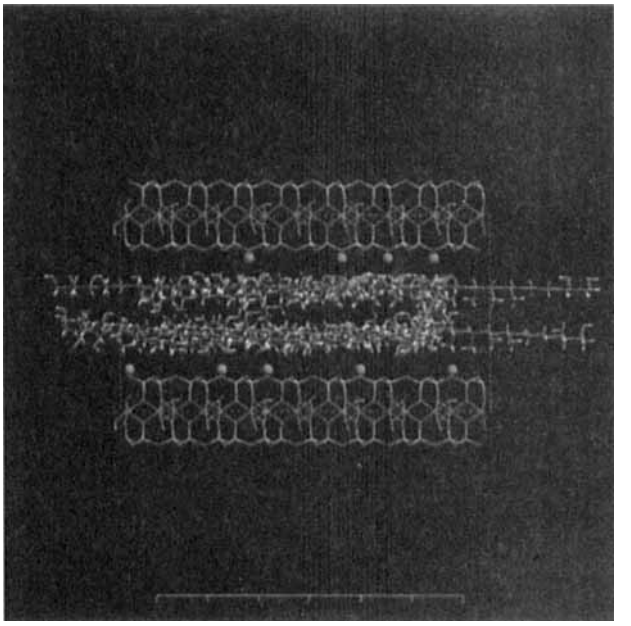

FIGURE 21 Snapshot from an equilibrated grand canonical MC simulation of 100% Biglotibros and sodium montmorillonite. (See Color Plate XVIII).

Downloaded At: 18:53 14 January 2011

terminally-hydroxylated compounds with respect to clay swelling will not be as great as for the sorbitol derivatives themselves, because of inadequate shielding of the hydroxyl-Na^+ interactions from those of water and Na^+. Thus the Na^+ ions can hydrate readily with free water molecules, and we expect that the clays will then swell as in the presence of water alone. This expectation is supported by some observations we have made on analogous polyalkylene diglucamides, which do *not* show strong inhibitory properties in aqueous solution [48]. There is also similar experimental evidence with Pluronic-style block polyalkylene glycols, for which those PAGs where the hydrophilic blocks are located on the exterior and the hydrophobic blocks on the interior are less effective clay swelling inhibitors than PAGs for which the converse holds [48].

5.3. Trends

The graphs in Figures 22–24 summarise several trends we have noted from our work. These figures show respectively plots of the final basal layer spacing *versus* molecular mass for intercalates in sodium montmorillonite,

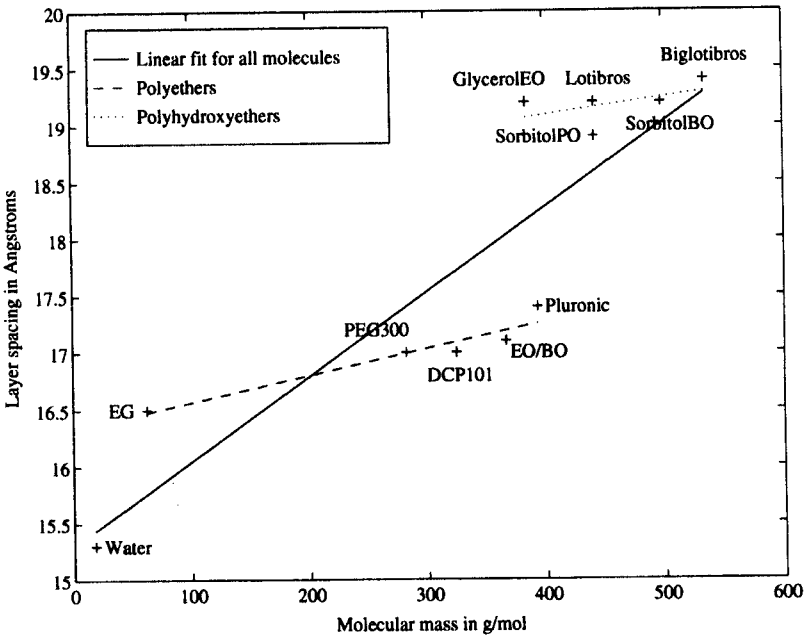

FIGURE 22 Final layer spacing *versus* molecular mass for sorbates in sodium montmorillonite.

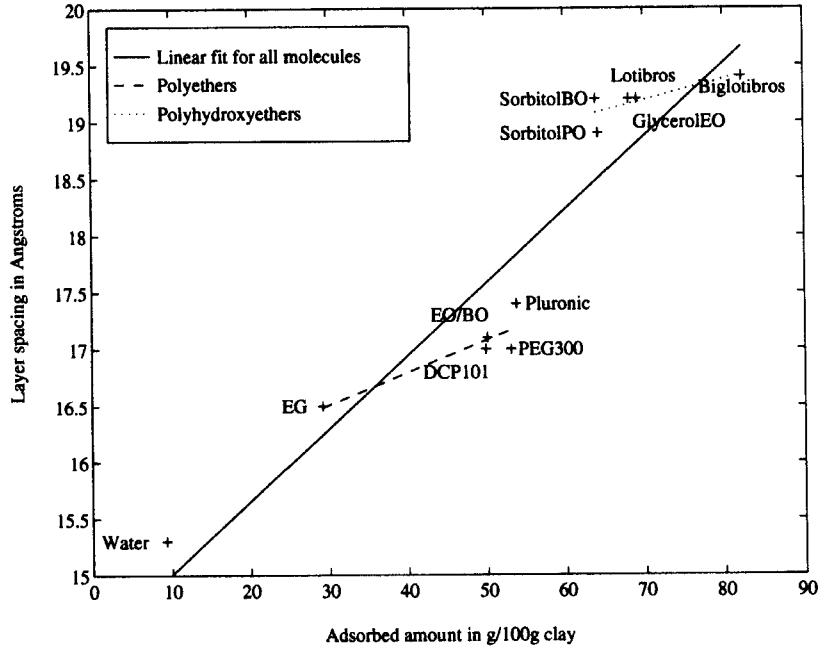

FIGURE 23 Final layer spacing *versus* (g/100 g clay) for sorbates in sodium montmorillonite.

Downloaded At: 18:53 14 January 2011

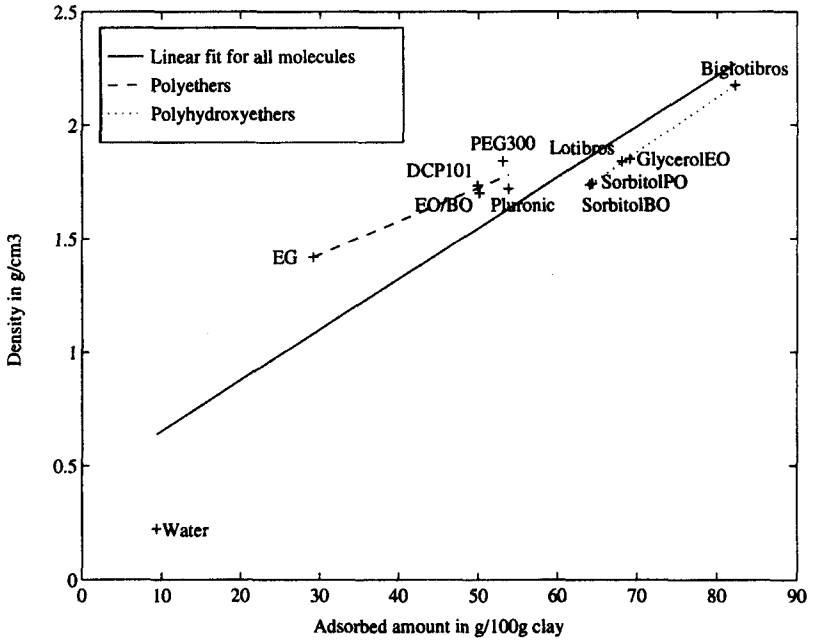

FIGURE 24 Sorbate density *versus* (g/100 g clay) for sorbates in sodium montmorillonite.

the final basal layer spacing *versus* (g/100 g clay) for intercalates in sodium montmorillonite, and sorbate density *versus* (g/100 g clay) for intercalates in sodium montmorillonite.

The most obvious thing that emerges from all three figures is that (excluding water which is included only for reference) the molecules fall into two distinct clusters. These clusters are the polyethers and the polyhydroxyethers. In the case of the polyethers, we know from our colleagues' experimental work that the order of improving clay-swelling inhibition properties is as follows:

$$\text{EG} < \text{PEG300} < \text{DCP101} < \text{EO/BO} < \text{Pluronic}.$$

This order is borne out well in Figure 22, which indicates that inhibition efficiency correlates with molecular mass. This is presumably because, in general terms, for molecules with the same kinds of atoms, the van der Waals forces themselves increase with molecular mass.

With respect to Figures 22 and 23, we should first make clear that a lower basal layer spacing does not necessarily indicate better inhibition. As the adsorption process during grand canonical Monte Carlo is carried out with a

Downloaded At: 18:53 14 January 2011

fixed layer spacing, the computed spacings come from post-Monte Carlo *NPT* molecular dynamics (see Section 3). As we previously discussed in the case of GlycerolEO (see Section 5.2.1), if intercalate adsorption is strong and its packing dense, it cannot be energetically favourable to reduce the layer spacing because of the many close interatomic contacts that would ensue. Indeed, we have even seen slight expansion of the basal spacing in some cases during MD because the amount of intercalate adsorbed is so high. Figure 23 shows clearly that basal layer spacing increases with amount adsorbed.

Consistent with this trend, we can see from Figure 22 that the polyhydroxyethers are significantly better inhibitors than the polyethers. We know this to be true from the empirical studies performed by the Drilling and Completion Fluids programme which indicates that in this case the order of increasing inhibition is as follows:

$$\text{GlycerolEO} < \text{SorbitolPO} < \text{SorbitolBO}.$$

This trend is shown in the figure, which also might be taken to imply that Lotibros should have similar inhibition properties to SorbitolPO, but that Biglotibros should exceed all of them. However, as noted earlier (Section 5.2.5), Lotibros and Biglotibros were not studied experimentally, and we have reasons to believe that they will be less effective at clay-swelling inhibition than the sorbitol derivatives, because of the important differences in the chemical structures which are not distinguished by the simulations that we have performed here (which were mainly on 100% pure reservoirs of the organic sorbates).

Generally speaking, we would expect that, as more intercalate is adsorbed, the density of the polymer after MD in the interlayer would also increase. To test this we studied the models after MD, and computed the density of the intercalates within the interlayer gallery. The results are displayed in Table X; indeed, the corresponding graph in Figure 24 gives a very good correlation, particularly for the polyhydroxyethers.

6. CONCLUSIONS

Using a range of computational techniques we have carried out a theoretical study of the inhibition of clay and shale swelling by polyethers and related compounds. By modelling known good and poor shale-swelling inhibitors, we have obtained qualitative and semi-quantitative insights which, for simple glycols and polyethers, are in general agreement with existing,

Downloaded At: 18:53 14 January 2011

empirical rules-of-thumb explaining the mechanism by which swelling is inhibited. In such cases, our results support the idea that the adsorption process is entropically dominated.

Building on the structures of the simpler compounds we studied initially, we have found that molecules with improved inhibitory performance possess well defined hydrophobic regions; for even greater effect, these molecules should also contain more polar (typically hydroxyl) groups embedded between the hydrophobic regions. Such molecules should be reasonably long chain linear organic molecules (oligomers) with significant hydrophobic and hydrophilic regions along the chain. The former provide a seal against ingress of water in water-based drilling fluid operations, and hence reduce wellbore damage, while the latter enhance the binding of the sodium cations to the clay surface, preventing hydration and the swelling that follows [1]. Indeed, it is possible in this way to find novel, environmentally friendly, water-based drilling-fluid additives that obviate the need for simultaneous inclusion of aqueous potassium chloride [48].

Summing up, the use of molecular modelling methods in combination with experimental observations has enabled us to enhance our understanding and prediction of the generic features of good clay-swelling inhibitors. Many other systems, which have not been reported here, have subsequently been studied and their observed behaviour can be interpreted on the basis of the same general principles described here.

Downloaded At: 18:53 14 January 2011

Acknowledgments

We are grateful to Bernadette Craster, John Crawshaw, Paul Reid and Neal Skipper for helpful discussions at various stages during this work.

References

[1] Boek, E. S., Coveney, P. V. and Skipper, N. T. (1995). "Monte Carlo molecular modelling studies of hydrated Li-, Na- and K-smectites: Understanding the role of potassium as a clay swelling inhibitor", *J. Am. Chem. Soc.*, **117**, 12608–12617.

[2] Boek, E. S., Coveney, P. V. and Skipper, N. T. (1995). "Molecular modelling of clay hydration: a study of hysteresis loops in the swelling curves of sodium montmorillonite, *Langmuir*, **11**, 4629–4631.

[3] Mooney, R. W., Keenan, A. G. and Wood, L. A. (1952). "Adsorption of water vapour by montmorillonite. 1. Heat of desorption and application of BET theory", *J. Am. Chem. Soc.*, **74**, 1367–1371.

[4] Brindley, G. W. and Brown, G. (1980). "*Crystal Structures of Clay Minerals and their X-ray Identification*", Minerological Society, London, Chapter 3.

[5] Keren, R. and Shainberg, I. (1975). *Clays Clay Miner.*, **23**, 193–200.

[6] Suquet, H., de la Calle, C. and Pezerat, H. (1975). *Clays Clay Miner.*, **23**, 1–9.

[7] Sato, T., Watanabe, T. and Otsuka, R. (1992). *Clays Clay Miner.*, **40**, 103–113.
[8] Cases, J. M., Berend, I., Besson, G., Francois, M., Uriot, J. P., Thomas, F. and Poirier, J. E. (1992). "Mechanism of adsorption and desorption of water vapour by homoionic montmorillonite. 1. Sodium exchanged form", *Langmuir*, **8**, 27830–2739.
[9] Zhang, Z. Z. and Low, P. F. (1989). "Relation between the heat of immersion and the initial water-content of Li-montmorillonite, Na-montmorillonite and K-montmorillonite", *J. Colloid Interface Sci.*, **133**, 461–472.
[10] Fu, M. H., Zhang, Z. Z. and Low, P. F. (1990). "Changes in the properties of a montmorillonite-water system during the adsorption and desorption of water-hysteresis", *Clays Clay Miner.*, **38**, 485–492.
[11] Sposito, G. and Prost, R. (1982). *Chem. Rev.*, **82**, 553–573.
[12] Pezerat, H. and Mering, J. (1967). *C. R. Acad. Sci. Paris (Serie D)*, **26**, 529–532.
[13] Ben Brahim, J., Besson, G. and Tchoubar, C. (1984). "Etudes des profils des bandes de diffraction X d'une Beidellite-Na Hydratée a deux couches d'Eau. Determination du mode d'empilement des feuillets et des sites occupés par l'eau", *J. Appl. Cryst.*, **17**, 179–188.
[14] Sposito, G., Prost, R. and Gaultier, J.-P. (1983). "Infrared spectroscopic study of adsorbed water on reduced-charge Na-Li-montmorillonites", *Clays Clay Miner.*, **31**, 9–16.
[15] Skipper, N. T., Soper, A. K. and McConnel, J. D. C. (1991). "The structure of interlayer water in vermiculite", *J. Chem. Phys.*, **94**, 5751–5760.
[16] Skipper, N. T., Soper, A. K. and Smalley, M. V. (1994). "Neutron-diffraction study of calcium vermiculite - hydration of calcium ions in a confined environment", *J. Phys. Chem.*, **98**, 942–945.
[17] Denis, J. H., Keall, M. J., Hall, P. L. and Meeten, G. H. (1991). "Influence of potassium concentration on the swelling and compaction of mixed (Na, K) ion-exchanged montmorillonite", *Clay Miner.*, **26**, 255–268.
[18] Low, P. F. (1987). "Structural component of the swelling pressure of clays", *Langmuir*, **3**, 18–25.
[19] Newman, A. C. D. (1987). "*Chemistry of Clays and Clay Minerals*", Minerological Society, London.
[20] Skipper, N. T., Sposito, G. and Chou Chang, F.-R. (1995). "Monte Carlo simulation of interlayer molecular structure in swelling clay-minerals. 2. Monolayer hydrates", *Clays Clay Miner.*, **43**, 294–303.
[21] Boek, E. S. and Coveney, P. V., unpublished work.
[22] Stewart, J. J. P., MOPAC Version 5.0, *QCPE No. 455* (Department of Chemistry, Indiana University, 1989).
[23] Mayo, S. L., Olafson, B. D. and Goddard, W. A. (1990). "A generic force field for molecular simulations", *J. Phys. Chem.*, **94**, 8897–8909.
[24] Cerius2 v1.6.2, *Molecular Simulations Inc.* (1995).
[25] Allen, M. P. and Tildesley, D. J. (1987). *Computer Simulation of Liquids*, Clarendon Press, Oxford.
[26] Metropolis, N., Rosenbluth, A. W., Rosenbluth, M. N., Teller, A. H. and Teller, E. (1953). "Equation of state calculations by fast computing machines", *J. Chem. Phys.*, **21**, 1087–1092.
[27] Cracknell, R. F., Nicholson, D., Parsonage, N. G. and Evans, H. (1990). "Rotational insertion bias: a novel method for simulating dense phases of structural particles, with particular application to water", *Mol. Phys.*, **71**, 931–943.
[28] Karaborni, S., Smit, B., Heidug, W., Urai, J. and van Oort, U. (1996). "The swelling of clays: Molecular simulations of the hydration of montmorillonite", *Science*, **271**, 1102–1104.
[29] Nose, S. J. (1984). "A unified formulation of the constant temperature molecular dynamics methods", *J. Chem. Phys.*, **81**, 511–519.
[30] Verlet, L. (1967). "Computer 'experiments' on classical fluids. I. Thermodynamical properties of Lennard–Jones molecules", *Phys. Rev.*, pp. 98–103.
[31] Skipper, N. T., Chou Chang, F.-R. and Sposito, G. (1995). "Monte Carlo simulations of interlayer molecular structure in swelling clay-minerals. 1. Methodology", *Clays Clay Miner.*, **43**, 285–293.

Downloaded At: 18:53 14 January 2011

[32] Chandraskhar, J., Spellmeyer, D. C. and Jorgensen, W. L. (1984). "Theoretical-study of silylene insertion into N—H, O—H, F—H, P—H, S—H and Cl—H bonds", *J. Am. Chem. Soc.*, **106**, 5858–5859.
[33] Briggs, J. M., Matsui, T. and Jorgensen, W. L. (1990). "Monte Carlo simulations of liquid alkyl ethers with the OPLS potential functions", *Comp. Chem.*, **11**, 958–971.
[34] Rappe, A., Casewit, C. J., Colwell, K. S., Goddard, III, W. A. and Skiff, W. M. (1992). "UFF: a full periodic-table, force-field for molecular mechanics and molecular dynamics simulations", *J. Am. Chem. Soc.*, **114**, 10024–10035.
[35] Boek, E. S., Coveney, P. V., Williams, S. J. and Bains, A. S. (1996). "A robust water potential parameterisation", *Molecular Simulation*, **18**, 145–154.
[36] Greenland, D. J. and Parfitt, R. L. (1970). "Adsorption of water by montmorillonite-poly(ethylene glycol) adsorption products", *Clay Miner.*, **8**, 317–324.
[37] Theng, B. K. G. (1979). "Formation and properties of clay-polymer complexes", *Developments in Soil Science*, Volume 9, Elsevier, Amsterdam, Netherlands.
[38] Craster, B. I. and Crawshaw, J., unpublished work.
[39] Reid, P. I., Dolan, B. I. and Cliffe, S., "Mechanism of shale inhibition by polyols in water based drilling fluids", SPE 28960 presented at "*SPE Int. Symp. Oilfield Chem.*", San Antonio, TX, USA, 14–17 February, 1995.
[40] Lewis, D. W., Freeman, C. M. and Catlow, C. R. A. (1995). "Predicting the templating ability of organic additives for the synthesis of microporous materials", *J. Phys. Chem.*, **99**, 11194–11202.
[41] Aicken, A. M., Bell, I. S., Coveney, P. V. and Jones, W. (1997). "Simulation of layered double hydroxide intercalates", *Advanced Materials*, **9**, 496–500.
[42] Aranda, P. and Ruiz-Hotzky, E. (1992). "Poly(ethylene oxide)-silicate intercalation materials", *Chem. Mater.*, **4**, 1395–1403.
[43] Wu, J. and Lerner, M. (1993). "Structural, thermal and electrical characterisation of layered nanocomposites derived from Na-montmorillonite and polyethylenes", *Chem. Mater.*, **5**, 835–838.
[44] Craster, B. I., unpublished work.
[45] Freeman, C. M., Catlow, C. R. A., Thomas, J. M. and Brode, S. (1991). "Computing the location and energetics of organic-molecules in microporous adsorbents and catalysts–a hybrid approach applied to isomeric butenes in a model zeolite", *Chem. Phys. Lett.*, **186**, 137–142.
[46] Shubin, A.-A., Catlow, C. R. A., Thomas, J. M. and Zamaraev, K. I. (1994). "A computational study of the adsorption of the isomers of butanal on silicatite and H-ZSM-5", *Proc. R. Soc. London Ser. A*, **446**, 411–427.
[47] Almgren, M., Brown, W. and Hvidt, S. (1995). "Self-aggregation and phase behaviour of poly(ethylene-oxide)poly(propylene-oxide)poly(ethylene-oxide) block-copolymers in aqueous solution", *Colloid Polym. Sci.*, **273**, 2–15.
[48] Boek, E. S., Coveney, P. V., Craster, B. I. and Reid, P. I. (1998). "Mechanisms of shale inhibition by polyglycol water-based muds and the development of improved additives through combined use of experimental and molecular modelling techniques", In: *Chemicals in the Oil Industry: Recent Developments*, Cookson, L. (Ed.), Royal Society of Chemistry Special Publication, **211**, 58–70.

Downloaded At: 18:53 14 January 2011